Eur. J. Mineral.
2005, **17**, 515-535

Two-, three- and four-feldspar assemblages with hyalophane and celsian: implications for phase equilibria in $BaAl_2Si_2O_8$–$CaAl_2Si_2O_8$–$NaAlSi_3O_8$–$KAlSi_3O_8$*

Eric J. ESSENE[1],**, Christopher L. CLAFLIN[2], Giovanna GIORGETTI[3],
Pilar M. MATA[4], Donald R. PEACOR[1], Péter ÁRKAI[5] and Mark A. RATHMELL[6]

[1]Department of Geological Sciences, University of Michigan, Ann Arbor MI 48109-1063 USA
[2]YES College Preparatory School, 353 Crenshaw Road, Houston TX 77034 USA
[3]Dipartimento di Scienze della Terra, Università di Siena, Via Laterina, 8, Italy
[4]Departmento de Geologia, Facultad de Ciencias del Mar, Universidad de Cadiz, Campus Rio San Pedro, 11510 Puerto Real, Cadiz, Spain
[5]Laboratory for Geochemical Research, Hungarian Academy of Sciences, H-1112 Budapest, Budaoersi ut 45, Hungary
[6]National Semiconductor, 234 Oxford Street, South Portland ME 04101 USA

Abstract: The occurrences of natural coexisting feldspars including hyalophane and also celsian delineate two-, three- and possibly four-phase fields in the system $BaAl_2Si_2O_8$–$CaAl_2Si_2O_8$–$NaAlSi_3O_8$–$KAlSi_3O_8$. Hyalophane occurs with albite and microcline in a very low grade (anchizonal to epizonal) metasedimentary association from the Uppony Mountains, Hungary, and in Grenville marbles from Ontario. Analyses show very little Ba in albite and only limited Na in hyalophane. One marble from the garnet zone has albite (Ab_{95-98}), oligoclase ($An_{17}Sl_3Ab_{80}$), hyalophane ($Cn_{65}Sl_3An_2Ab_9Or_{24}$) and celsian ($Cn_{92}Sl_3An_1Ab_2Or_2$). The albite and oligoclase are complexly intergrown and may indicate unmixing during cooling. A marble in the sillimanite zone contains albite ($Ab_{95-98}Or_{2-3}$), oligoclase ($An_{17}An_2Sl_3Ab_{33}Or_{24}$), hyalophane ($Cn_{65}Sl_3An_2Ab_9Or_{24}$), and an inclusion of celsian ($Cn_{67}An_1Sl_2Ab_2Or_{91}$) in an albite. Sanidine from the Peshtigo monzonite in Wisconsin unmixed to a symplectic perthite with barian microcline ($Cn_{8-11}An_2Ab_{8-13}Or_{75-80}$) and oligoclase ($Cn1An_{18}Ab_{79}Or_2$). The former compositions of the ternary igneous feldspars ($Cn_3An_9Ab_{46}Or_{42}$, $Cn_1An_{18}Ab_{69}Or_{12}$) were obtained by reintegration.

The Na content of hyalophane equilibrated with albite is correlated with metamorphic grade. Hyalophane has 5 ± 2 mol % Ab in very low-grade associations, 10 ± 3 mol % Ab in the greenschist facies, 16 ± 2 mol % Ab in the low to middle amphibolite facies, and 30 mol % Ab in the upper amphibolite to granulite facies even when not buffered with albite. The limited Na content of celsian equilibrated with albite in the greenschist facies is in striking disagreement with the narrow solvi obtained from unreversed experiments on the join $BaAl_2Si_2O_{86}$–$NaAlSi_3O_8$.

Up to 8 four-feldspar and 24 three-feldspar assemblages may be stable in the system $BaAl_2Si_2O_8$–$CaAl_2Si_2O_8$–$NaAlSi_3O_8$–$KAlSi_3O_8$. In contrast, the repeatedly observed and variably located discontinuities within zoned hyalophane grains may represent changes in the environment during mineral growth rather than internal miscibility gaps. Given its miscibility gaps with microcline and celsian, the name hyalophane is justified for intermediate feldspars near the Cn-Or join.

Key-words: hyalophane, celsian, solvus, three feldspars, four feldspars, $BaAl_2Si_2O_8$–$NaAlSi_3O_8$–$KAlSi_3O_8$, $BaAl_2Si_2O_8$–$CaAl_2Si_2O_8$–$NaAlSi_3O_8$–$KAlSi_3O_8$

Introduction

Most natural feldspars are well represented compositionally in $CaAl_2Si_2O_8$–$NaAlSi_3O_8$–$KAlSi_3O_8$ (An–Ab–Or). However, barian feldspars occur sporadically in diverse settings ranging from diagenetically altered sediments and hydrothermal veins, to marbles and other metasediments, to granites, pegmatites and felsic volcanic rocks. Celsian (Cn, $BaAl_2Si_2O_8$) has a structure similar to that of anorthite but with significant Al and Si disorder (Griffen & Ribbe, 1976). It has a polymorph, paracelsian, with a different space group, isostructural with danburite ($CaB_2Si_2O_8$) (Chiari *et al.*, 1985), slawsonite (Sl, $SrAl_2Si_2O_8$) (Griffen *et al.*, 1977), also meleevite ($BaB_2Si_2O_8$) and pekovite ($SrB_2Si_2O_8$) (Pautov *et al.*, 2004). Lin & Foster (1968) reacted paracelsian to celsian at T ≥ 500°C and 1 kbar and concluded that paracelsian is metastable. A stability field for paracelsian cannot however be ruled out altogether at

---

*Contribution No. 518 from the Mineralogical Laboratory, Department of Geological Sciences, The University of Michigan 48109-1063.
**E-mail: essene@umich.edu

0935-1221/05/0017-0515 $ 9.45

DOI: 10.1127/0935-1221/2005/0017-0515

Table 1. Assemblages in rocks with barian feldspars.

sample #	*Ba feldspar(s)*	*other feldspars*	*quartz*	*ferromag silicates*	*other minerals (in decreasing order of abundance)*
S. Ontario					
KA901B	hyalophane*	Ab	x	phlogopite*	Cc, Mu*, Brt*, Fl, Sph, Dol, Ap, C, Ru, Py, Po, Ahy, Zc, [Wth*]
KA914A	+celsian*	Ab, Kfs	x	phlogopite*	Cc, Fl, Sph, Brt*, Dol, Py, C, (Ru)
BA904A	K-feldspar*	--	(x)	phlogopite*, tremolite	Cc, Di, Dol, Sph, Ap, Cl-Ap, C, Thor, Po, (Ru), (Py)
BB9224	hyalophane*, celsian*	Ab, Olig, [Kfs]	x	phlogopite*	Cc, Mu*, Pg, Sph, Py, Ap, Ru, C, Zc, (Dol), +BC*
Uppony Mtns.					
Dt-8 207.8 m	hyalophane*	Ab, Kfs	x	chlorite	Cc, Py, Ru, Zc
C. Wisconsin					
92-ATC	K-feldspar*	Ab	x	Fa, Hb, Hyp, Bi	Ap, Fl, Zc, All, Il, Mt

*Barian phases (> 1 wt % BaO).

+Single inclusion identified in an albite porphyroblast.

Abbreviations:

Ab = albite, Ahy = anhydrite, All = allanite, Ap = (F,OH)-apatite, Brt = barite, BC = barytocalcite, Bi = biotite, C = graphite, Cc = calcite, Cl-Ap = chlorapatite, Dol = dolomite, Fa = fayalite, Fl = fluorite, Hb = hornblende, Hyp = hypersthene, Il = ilmenite, Kfs = K-feldspar, Mt = magnetite, Mu = muscovite, Olig = oligoclase, Pg = paragonite, Po = pyrrhotite, Py = pyrite, Ru = rutile, Sph = sphene, Thor = thorite, Wth = witherite, Zc = zircon.

Phases in parentheses were identified by Rathmell (1993) but not found in a second thin section from the same rock by EJE.

Phase in square brackets are inferred to have formed during retrograde alteration.

lower T. Slawsonite is thought to react to Sr feldspar above 600°C (Bambauer & Nager, 1981), although the reaction has not been reversed.

Unlike anorthite, celsian forms extensive solid solution with K-feldspar, and the intermediate phase is designated as hyalophane (Hy). Most hyalophane compositions are in the range from Cn_{10} to Cn_{50} with the remainder represented by major Or and minor Ab (Deer *et al.*, 2001). The necessity of a separate mineral name for hyalophane is not obvious from a perusal of the literature and will be reviewed in this paper. Gay & Roy (1968) found that hyalophane with < 30 % Cn is triclinic. However, Viswanathan & Kielhorn (1983a) obtained the cell parameters of 20 samples of hyalophane from Otosondu, Namibia, and found that nearly all were monoclinic. Viswanathan & Kielhorn (1983b) determined from a crystal structure refinement that a ternary hyalophane ($Cn_{40}Ab_{13}Or_{47}$) was monoclinic and partially disordered in terms of its Al and Si distribution.

Observations of solid solutions and the compositions of coexisting phases from metamorphic rocks provide valuable information on phase equilibria. This approach has provided insights for the phase equilibria of pyroxenoids and pyroxenes (Brown *et al.*, 1981; Petersen *et al.*, 1984), rhombohedral carbonates (Essene, 1983; Anovitz & Essene, 1987), and orthorhombic carbonates (Boundy *et al.*, 2002). Some experiments are available in the system $BaAl_2Si_2O_8$–$NaAlSi_3O_8$–$KAlSi_3O_8$, but they have not been applied systematically to natural assemblages. Barian feldspar assemblages have therefore been evaluated in this paper.

Geological settings

Three different hyalophane associations were studied and are described herein. Coexisting minerals for samples from each association are listed in Table 1. A complex hyalophane assemblage has been identified in an epizonal metasandstone from the Tapolcsány Formation of the Uppony Mountains (Bükkium, NE Hungary). This Early Paleozoic (Silurian?) sequence of sediments underwent a regional metamorphism of a collisional type in the Cretaceous (*ca.* 95-105 Ma). On the basis of illite "crystallinity", white K-mica *b* geobarometry and coal rank data, metamorphism is inferred to be a low-P type with a T maximum of *ca.* 300-350°C (Árkai *et al.*, 1981, 1995, 2000; Árkai, 1983). The sediment investigated in detail was sampled at 207.8 m depth from borehole Dt-8 in the village of Dédestapolcsány. Younger, low-temperature hydrothermal fluids that caused Fe-Mn metasomatism in carbonates extensively affected the rock (Polgári & Fórizs, 1996). Corrensite and randomly interstratified chlorite/smectite observed by TEM are products of retrogression related to post-metamorphic hydrothermal activity (Árkai *et al.*, 2000). The sediments contain complex intergrowths K-feldspar, albite and hyalophane.

Barian assemblages were identified in four of the 80 Grenville marbles investigated by Rathmell (1993). The Grenville rocks in this area of southern Ontario were metamorphosed around 1.17 Ga ago subsequent to deposition on a continental shelf and followed by metamorphism during continent-continent collision (Cosca *et al.*, 1992; Mezger *et al.*, 1993). The feldspars occur as serrated,

Table 2. Electron microprobe analyses of feldspars from Uppony Mountain, Hungary*.

°*phase*	Hy	Hy	Hy	Hy	Hy	Hy	Hy	Hy	Kfs	Kfs	Kfs	Kfs	Kfs	Ab	Ab
**analyst*	EJE	EJE	EJE	EJE	EJE	EJE	EJE	EJE	EJE	EJE	EJE	EJE	EJE	EJE	EJE
SiO_2	52.97	52.87	52.99	52.83	51.96	53.13	55.76	55.69	63.53	64.77	66.44	65.52	65.01	70.27	70.63
TiO_2	0.00	0.18	0.00	0.00	0.00	0.00	0.00	0.00	0.00	0.00	0.00	0.00	0.00	0.00	0.00
Al_2O_3	21.91	21.91	21.90	21.87	22.14	22.05	20.92	20.93	18.80	18.78	18.98	18.66	18.61	19.84	19.82
Fe_2O_3	0.34	0.43	0.06	0.07	0.14	0.19	0.16	0.00	0.11	0.03	0.01	0.01	0.01	0.10	0.10
CaO	0.00	0.01	0.09	0.16	0.12	0.00	0.00	0.00	0.00	0.00	0.00	0.00	0.00	0.04	0.04
BaO	15.60	15.58	16.10	16.17	16.64	15.99	11.82	12.26	1.20	1.93	1.95	1.57	1.48	0.00	0.01
Na_2O	0.57	0.62	0.49	0.48	0.51	0.44	0.70	0.46	1.39	0.36	0.32	0.46	0.45	11.51	10.43
K_2O	9.22	9.06	9.25	9.29	8.99	9.18	10.48	10.38	14.39	14.79	13.50	15.56	15.36	0.06	0.07
sum	100.61	100.65	100.87	100.87	100.50	100.98	99.84	99.72	99.41	100.66	101.20	101.78	100.91	101.81	101.08
Si	2.695	2.690	2.692	2.688	2.666	2.694	2.779	2.780	2.967	2.990	3.018	2.995	2.994	3.009	3.030
Al	1.314	1.314	1.311	1.311	1.339	1.317	1.229	1.231	1.035	1.022	1.016	1.005	1.010	1.001	1.002
Fe	0.014	0.018	0.002	0.003	0.006	0.008	0.007	0.000	0.004	0.001	0.000	0.000	0.000	0.003	0.003
Ti	0.000	0.007	0.000	0.000	0.000	0.000	0.000	0.000	0.000	0.000	0.000	0.000	0.000	0.000	0.000
Ca	0.000	0.000	0.005	0.009	0.006	0.000	0.000	0.000	0.000	0.000	0.000	0.000	0.000	0.002	0.002
Ba	0.311	0.311	0.321	0.322	0.335	0.318	0.231	0.240	0.022	0.035	0.035	0.028	0.027	0.000	0.000
Na	0.056	0.061	0.048	0.047	0.051	0.043	0.068	0.045	0.126	0.032	0.029	0.040	0.040	0.956	0.867
K	0.599	0.588	0.599	0.603	0.588	0.594	0.667	0.661	0.857	0.871	0.782	0.908	0.902	0.003	0.004
sum	4.989	4.989	4.978	4.984	4.990	4.974	4.980	4.957	5.011	4.952	4.880	4.977	4.973	4.974	4.908
Cn	32.2	32.3	33.0	32.8	34.1	33.3	23.9	25.4	2.2	3.7	4.1	2.9	2.8	0.0	0.0
An	0.0	0.0	0.5	0.9	0.7	0.0	0.0	0.0	0.0	0.0	0.0	0.0	0.0	0.2	0.2
Ab	5.8	6.4	4.9	4.8	5.2	4.6	7.0	4.7	12.5	3.4	3.4	4.1	4.1	99.5	99.4
Or	62.0	61.2	61.6	61.4	60.0	62.2	69.1	69.9	85.3	92.9	92.5	93.0	93.1	0.3	0.4

°Abbreviations: Ab-albite, An-anorthite, Cn-celsian, Hy-hyalophane, Kfs-Kfeldspar, Or-orthoclase, Sl-slawsonite.
*Analyst EJE = E.J. Essene.

rounded, and subhedral grains with low birefringence in a calcite matrix. Albite is distinguished from coexisting hyalophane and oligoclase by its positive sign in thin section, which also indicates that it is ordered. The celsian is too small for an optical interference figure, but it is not macroscopically twinned, suggesting that it is celsian rather than paracelsian (Deer *et al.,* 2001). The association of fluorite, anhydrite, barite and witherite is unusual, although thick anhydrite beds are associated underground in Grenville marbles at Balmat, NY. The senior author has identified accessory barite in marble outcrops on Monck Road, 2 km E of Cardiff and 13 km W of Bancroft, Ontario, and barite and celestite solid solutions in a marble breccia from a large road outcrop on Rt. 35, 0.3 km N of Miners Bay, Ontario.

Two barian marbles (KA901B, KA914A) of this study come from a single outcrop of graphitic marble located just N of Madoc, Ontario, on Route 62 one km N of its intersection with Route 7. Nearby metapelite assemblages and P-T measurements on both marbles and metapelites indicate that these rocks attained the garnet zone of the greenschist facies at 480 ± 20°C and 3-4 kbar (Rathmell *et al.*, 1999). A third assemblage (BA904A) was collected 5.0 km SE of Bancroft on Rt. 62, and a fourth (BB9224) 18.5 km S of Coe Hill on Rt. 46. The latter two assemblages occur just upgrade from the first sillimanite isograd of the amphibolite facies at 550-600°C and 5-6 kbar (Streepey *et al.*, 1997).

Striking intergrowths of barian microcline and oligoclase that unmixed from barian sanidine and barian oligoclase were found in the Peshtigo monzonite from Central Wisconsin (Claflin, 2001). These rocks are part of a mid-Proterozoic (1.6 Ga) Rapikivi granite suite (Anderson, 1980; Anderson *et al.*, 1980). The rocks are also enriched in F and REE as shown by the presence of igneous fluorite and allanite.

Analytical methods

Polished thin sections of the samples were prepared for optical and back-scattered electron imaging using the scanning electron microscope (SEM) and electron microprobe (EMP). Identification of Ba-rich areas is made easy using back-scattered electron (BSE) imaging by their high atomic number compared to matrix calcite, dolomite, albite, phlogopite, K-feldspar and quartz. The EMP analyses of MAR and some of those by EJE were obtained on the Univ. of Michigan Cameca MBX, and those of CLC and others of EJE were conducted on the Univ. of Michigan Cameca SX-100. Standards used with X-ray lines in parentheses are: Tiburon albite (Na *K*α), St. Gotthard K-feldspar (K, Si *K*α), Tanzania tanzanite (Ca, Al *K*α), Ingamells almandine (Fe *K*α), Ohio celestite (Sr *L*α), and Mariposa Co. sanbornite (Ba *L*α). The background interference between Sr and Si was minimized by using a PET crystal and wavelength scans were employed to select the position of the long wavelength background. Cameca PAP corrections were applied, with oxygen calculated by stoichiometry assuming all iron as ferric. Analytical results are provided in Tables 2-7, where the feldspars are normalized to

Table 3. Electron microprobe analyses of feldspars from Grenville marble near Madoc, Ontario (KA901B).

sample								core	rim	adj	adj	adj
°phase	Hy	Hy	Hy	Hy	Hy	Hy	Hy	Hy	Hy	Hy	Ab	Or
*analyst	MAR	MAR	MAR	MAR	MAR	EJE	EJE	EJE	EJE	EJE	EJE	EJE
SiO_2	48.95	54.34	48.08	50.43	54.33	49.43	56.66	53.05	54.73	52.30	66.93	71.61
Al_2O_3	21.85	20.58	21.68	21.59	20.89	22.09	21.01	21.85	21.54	22.26	20.95	17.53
Fe_2O_3	0.00	0.00	0.06	0.00	0.02	0.04	0.13	0.07	0.10	0.15	0.03	0.00
CaO	0.74	0.27	0.40	0.38	0.41	0.54	0.48	0.35	0.42	0.35	1.49	1.10
SrO	--	--	--	--	--	--	0.10	0.18	0.18	0.14	0.18	0.12
BaO	18.18	11.99	18.64	16.82	12.40	18.39	11.46	12.69	12.69	15.00	0.03	0.00
Na_2O	1.13	1.24	0.77	0.79	0.90	0.8	1.38	1.08	1.08	0.72	11.05	9.63
K_2O	7.41	10.04	7.79	8.41	10.01	7.89	9.92	9.70	9.60	9.24	0.05	0.00
sum	98.26	98.46	97.42	98.42	98.96	99.18	101.14	98.97	100.34	100.16	100.71	99.99
Si	2.606	2.757	2.599	2.651	2.748	2.609	2.775	2.695	2.730	2.664	2.920	2.959
Al	1.371	1.231	1.381	1.338	1.245	1.374	1.213	1.308	1.267	1.336	1.077	1.037
Fe	0.000	0.000	0.002	0.000	0.001	0.002	0.005	0.003	0.004	0.006	0.001	0.000
Ca	0.042	0.015	0.023	0.021	0.022	0.031	0.025	0.019	0.022	0.019	0.070	0.004
Sr	--	--	--	--	--	--	0.003	0.005	0.005	0.004	0.005	--
Ba	0.379	0.238	0.395	0.347	0.246	0.380	0.220	0.253	0.248	0.299	0.001	0.046
Na	0.117	0.122	0.081	0.081	0.088	0.082	0.131	0.106	0.104	0.071	0.935	0.092
K	0.503	0.650	0.537	0.564	0.646	0.531	0.620	0.628	0.611	0.600	0.003	0.860
sum	5.018	5.013	5.018	5.002	4.996	5.009	4.991	5.017	4.992	5.001	5.010	4.998
Cn	36.4	23.3	38.1	34.2	24.5	37.1	22.0	25.0	25.0	30.1	0.1	4.6
An	4.1	1.4	2.2	2.1	2.2	3.0	2.5	1.9	2.3	1.9	6.9	0.4
Sl	--	--	--	--	--	--	0.3	0.5	0.5	0.4	0.4	--
Ab	11.2	11.9	7.8	8.0	8.8	8.0	13.1	10.5	10.5	7.2	92.3	9.2
Or	48.3	63.4	51.9	55.7	64.5	51.9	62.1	62.1	61.6	60.4	0.3	85.8

0.1 indicates an individual grain, c = core, r = rim.
°Abbreviations: Ab - albite, An - anorthite, Cn - celsian, Kfs - K feldspar, Or - orthoclase, Sl - slawsonite.
*Analyst: MAR = M.A. Rathmell, EJE = E.J. Essene.

Table 4. Electron microprobe analyses of feldspars from Grenville marble near Madoc, Ontario (KA914A).

°phase	Cn	Cn	Cn	eu Cn	late Kfs	repl Cn	Ab	Ab	Cn rim	Hy rim	Hy rim
*analyst	MAR	MAR	MAR	EJE	EJE	EJE	EJE	EJE	EJE	EJE	EJE
SiO_2	30.79	30.88	32.00	31.77	62.87	31.08	68.16	66.86	32.85	40.65	39.42
Al_2O_3	25.83	25.78	25.73	26.57	19.01	26.80	20.08	21.37	27.22	24.75	25.15
Fe_2O_3	0.02	0.02	0.00	0.01	0.05	0.16	0.04	0.00	0.1	0.04	0.03
CaO	1.63^{+}	2.55^{+}	1.21^{+}	0.40	0.35	0.40	0.37	1.50	0.19	0.24	0.26
SrO	--	--	--	0.09	0.05	0.01	0.01	0.33	1.09	0.95	0.91
BaO	39.98	38.95	39.27	39.84	1.96	40.68	0.00	0.04	37.81	28.58	29.85
Na_2O	0.18	0.20	0.35	0.23	0.09	0.16	11.72	10.86	0.22	0.83	0.74
K_2O	0.14	0.20	0.27	0.20	15.71	0.22	0.03	0.03	0.26	3.17	2.74
sum	98.57	98.58	98.83	99.10	100.08	99.52	100.41	100.99	99.74	99.21	99.10
Si	1.971	1.966	2.021	2.002	2.947	1.967	2.969	2.909	2.022	2.324	2.280
Al	1.949	1.934	1.915	1.973	1.050	1.999	1.031	1.096	1.975	1.668	1.715
Fe	0.001	0.001	0.000	0.000	0.002	0.008	0.001	0.000	0.005	0.002	0.001
Ca	0.112^{+}	0.174^{+}	0.082^{+}	0.027	0.018	0.027	0.017	0.070	0.013	0.015	0.016
Sr	0.000	0.000	0.000	0.003	0.001	0.000	0.000	0.008	0.039	0.031	0.031
Ba	1.003	0.972	0.972	0.984	0.036	1.009	0.000	0.001	0.912	0.640	0.677
Na	0.022	0.025	0.043	0.028	0.008	0.020	0.990	0.916	0.026	0.092	0.083
K	0.011	0.016	0.022	0.016	0.939	0.018	0.002	0.002	0.020	0.231	0.202
sum	5.070	5.087	5.054	5.034	5.001	5.048	5.010	5.002	5.012	5.003	5.004
Cn	87.3	81.9	86.9	93.0	3.6	94.0	0.0	0.1	90.3	63.4	67.1
An	9.7^{+}	14.7^{+}	7.3^{+}	2.6	1.8	2.5	1.7	7.0	1.2	1.5	1.6
Sl	0.0	0.0	0.0	0.3	0.1	0.0	0.0	0.8	3.9	3.1	3.0
Ab	1.9	2.1	3.8	2.7	0.8	1.8	98.1	91.9	2.6	9.1	8.2
Or	1.0	1.4	1.9	1.5	93.7	1.7	0.2	0.2	2.0	22.9	20.1

°Abbreviations: Ab - albite, An - anorthite, Cn - celsian, Kfs - K feldspar, Or - orthoclase, Sl - slawsonite.
*Analyst: MAR = M.A. Rathmell, EJE = E.J. Essene. $^{+}$high Ca probably an artifact of matrix fluorescence.

Table 5. Electron microprobe analyses of feldspars from Grenville marbles near Bancroft, Ontario (BA904A).

phase	Hy	Hy	Hy	Hy	Hy	Hy	Hy	Hy	Hy	Hy core	Hy rim	Hy core	Hy rim 1	Hy rim 2	Hy rim 3
*analyst	MAR	MAR	MAR	MAR	MAR	MAR	MAR	MAR	MAR	EJE	EJE	EJE	EJE	EJE	EJE
SiO_2	58.14	62.03	62.02	58.06	60.67	61.30	63.11	63.11	63.11	63.83	60.30	64.72	62.57	60.98	59.19
Al_2O_3	20.48	18.54	18.32	19.39	19.05	19.02	18.77	18.77	18.77	19.22	20.06	18.98	19.45	20.00	20.07
Fe_2O_3	0.00	0.00	0.05	0.03	0.00	0.00	0.00	0.00	0.00	0.00	0.04	0.03	0.08	0.00	0.02
CaO	0.01	0.01	0.01	0.03	0.02	0.03	0.07	0.07	0.07	0.00	0.09	0.05	0.06	0.05	0.04
SrO	--	--	--	--	--	--	--	--	--	0.00	0.03	0.00	0.00	0.02	0.00
BaO	6.76	2.68	1.96	6.78	4.64	4.10	2.53	2.53	2.53	2.23	6.36	1.34	3.49	5.59	7.35
Na_2O	0.82	0.87	0.85	0.95	0.96	1.02	1.01	1.01	1.01	0.86	0.93	0.92	0.85	0.89	0.95
K_2O	10.57	14.59	14.85	12.89	13.20	13.78	14.37	14.37	14.37	14.97	13.34	15.04	14.26	13.55	12.96
sum	98.05	98.72	98.06	98.13	98.54	99.25	99.86	99.86	99.86	101.10	101.14	101.08	100.76	101.08	100.58
Si	2.866	2.953	2.961	2.862	2.920	2.925	2.959	2.959	2.959	2.954	2.869	2.974	2.928	2.885	2.853
Al	1.128	1.040	1.031	1.127	1.081	1.070	1.037	1.037	1.037	1.048	1.125	1.028	1.073	1.115	1.140
Fe	0.000	0.000	0.002	0.001	0.000	0.000	0.000	0.000	0.000	0.000	0.001	0.001	0.003	0.000	0.001
Ca	0.001	0.001	0.001	0.002	0.001	0.002	0.004	0.004	0.004	0.000	0.005	0.002	0.003	0.003	0.002
Sr	--	--	--	--	--	--	--	--	--	0.000	0.001	0.000	0.000	0.001	0.000
Ba	0.131	0.050	0.037	0.131	0.088	0.077	0.046	0.046	0.046	0.040	0.119	0.024	0.064	0.104	0.139
Na	0.078	0.080	0.079	0.091	0.090	0.094	0.092	0.092	0.092	0.077	0.086	0.082	0.077	0.082	0.089
K	0.811	0.886	0.904	0.811	0.811	0.839	0.860	0.860	0.860	0.884	0.810	0.882	0.851	0.818	0.797
sum	5.015	5.010	5.014	5.024	4.990	5.006	4.998	4.998	4.998	5.003	5.015	4.993	4.999	5.007	5.020
Cn	12.8	4.9	3.6	12.7	8.9	7.6	4.6	4.6	4.6	4.0	11.7	2.4	6.4	10.3	13.5
An	0.1	0.1	0.1	0.2	0.1	0.2	0.4	0.4	0.4	0.0	0.5	0.2	0.3	0.3	0.2
Sl	--	--	--	--	--	--	--	--	--	0.0	0.1	0.0	0.0	0.1	0.0
Ab	7.7	7.9	7.7	8.8	9.1	9.3	9.2	9.2	9.2	7.7	8.5	8.3	7.7	8.2	8.7
Or	79.5	87.1	88.6	78.4	82.0	82.9	85.8	85.8	85.8	88.3	79.2	89.1	85.6	81.1	77.6

°Abbreviations: Ab - albite, An - anorthite, Cn - celsian, Hy - hyalophane, Or - orthoclase, Sl - slawsonite.

*Analyst: MAR = M.A. Rathmell, EJE = E.J. Essene.

Table 6. Electron microprobe analyses of feldspars from Grenville marbles near Coe Hill, Ontario (BA9224).

sample	BB9224.0	BB9224.1	BB9224.1	BB9224.1	BB9224.2	BB9224.2	BB9224.3	BB9224.3	BB9224.3	BB9224.4	BB9224.4	BB9224.4
phase	Hy	Hy incl	Ab host	Hy incl	Hy core	Hy rim	Ab	Ab	XCn incl	lo Z Ab	hi Z Ab	Cn rim
oxide wt%	*MAR	*EJE	EJE	EJE	EJE	EJE	EJE	EJE	EJE	EJE	EJE	EJE
SiO_2	55.09	44.23	66.63	46.53	54.66	48.72	67.51	67.45	37.98	66.48	65.51	33.79
Al_2O_3	20.56	24.85	20.11	22.86	20.88	20.78	19.75	21.37	24.74	20.30	20.76	26.99
Fe_2O_3	0.00	0.02	0.00	0.01	0.00	0.00	0.00	0.00	0.00	0.00	0.00	0.10
CaO	0.05	0.13	0.61	0.20	0.02	0.14	0.25	1.10	0.14	0.80	1.26	0.19
SrO	--	0.44	0.33	0.08	0.35	0.28	0.11	0.33	0.70	0.56	0.67	1.09
BaO	11.28	24.75	0.10	21.57	12.19	18.64	0.00	0.04	31.28	0.03	0.02	38.81
Na_2O	1.64	0.99	11.26	0.56	1.44	1.17	11.85	10.86	0.44	11.09	10.66	0.22
K_2O	9.61	5.01	0.03	7.36	9.48	7.47	0.00	0.03	1.22	0.01	0.02	0.26
sum	98.23	100.43	99.08	99.15	99.02	98.41	99.47	101.18	98.04	99.26	98.90	99.48
Si	2.777	2.601	2.951	2.525	2.756	2.601	2.972	2.932	2.248	2.942	2.915	2.031
Al	1.221	1.384	1.050	1.462	1.241	1.384	1.024	1.091	1.725	1.059	1.089	1.950
Fe	0.000	0.000	0.000	0.000	0.000	0.000	0.000	0.000	0.000	0.000	0.000	0.005
Ca	0.003	0.010	0.029	0.012	0.001	0.008	0.012	0.051	0.009	0.038	0.060	0.012
Sr	--	0.014	0.010	0.002	0.010	0.009	0.003	0.008	0.024	0.014	0.017	0.039
Ba	0.223	0.407	0.002	0.459	0.241	0.390	0.000	0.001	0.725	0.001	0.000	0.932
Na	0.160	0.092	0.967	0.059	0.141	0.121	1.011	0.912	0.229	0.951	0.920	0.026
K	0.618	0.520	0.002	0.509	0.610	0.509	0.003	0.002	0.092	0.000	0.001	0.020
sum	5.002	5.013	5.009	5.027	4.999	5.022	5.022	4.988	5.051	5.005	5.002	5.015
Cn	22.2	39.6	0.2	44.0	24.0	37.6	1.2	0.1	65.8	0.1	0.0	90.5
An	0.3	1.0	1.0	1.2	0.1	0.8	1.2	5.1	0.9	3.8	6.0	1.2
Sl	--	1.4	1.0	0.2	1.0	0.8	0.3	0.8	2.4	1.4	1.7	3.8
Ab	16.0	8.9	97.6	5.9	14.0	11.7	97.0	94.8	20.8	94.7	92.2	2.5
Or	61.6	50.6	0.2	48.7	60.8	49.1	0.3	0.2	9.2	0.0	0.1	2.0

Number following decimal indicates individual grain in thin section.

°Abbreviations: Ab - albite, An - anorthite, Cn - celsian, Hy - hyalophane, Kfs - K feldspar, Or - orthoclase, Sl - slawsonite.

*Analyst MAR = M.A. Rathmell, EJE = E.J. Essene.

+10 μm celsian inclusion in albite.

Table 7. Electron microprobe analyses of feldspars from the Peshtigo monzonite near Keshena, Wisconsin

sample	14	14	14	14	14	14	15	15	15	15	15	16	16	16	16	16	16
phase	Kfs core	Kfs core	Kfs rim	Pg core	Plg rim	Plg rim	Kfs rim	Kfs rim	Pg core	Pg rim	Pg rim	Kfs core	Kfs rim	Kfs rim	Pg core	Pg rim	Pg rim
**analyst*	CLC	CLC	CLC	CLC	CLC	CLC	CLC	CLC	CLC	CLC	CLC	CLC	CLC	CLC	CLC	CLC	CLC
SiO_2	64.20	63.51	63.78	64.19	63.11	63.73	63.93	61.81	63.21	63.57	63.92	62.86	62.00	62.12	63.30	62.81	62.72
Al_2O_3	19.66	19.39	19.05	23.05	22.97	23.02	19.27	18.82	22.65	23.45	23.23	19.12	19.32	19.00	21.80	22.68	22.30
Fe_2O_3	0.10	0.07	0.15	0.15	0.01	0.10	0.12	1.85	0.04	0.05	0.06	0.06	0.02	0.11	0.04	0.07	0.12
CaO	0.46	0.07	0.06	4.06	4.40	4.08	0.12	0.10	3.11	4.17	3.92	0.07	0.00	0.00	3.07	4.29	3.92
SrO	0.00	0.00	0.16	0.04	0.02	0.10	0.00	0.06	0.11	0.03	0.04	0.02	0.01	0.00	0.00	0.00	0.01
BaO	2.30	3.01	1.39	0.01	0.02	0.02	2.54	2.78	0.33	0.00	0.02	2.60	3.92	3.47	0.47	0.05	0.07
Na_2O	3.25	1.83	1.54	8.34	8.97	9.18	2.32	1.77	7.55	9.32	9.47	1.59	1.67	1.59	9.04	9.41	9.16
K_2O	10.93	13.07	13.95	1.28	0.17	0.13	12.56	12.63	3.56	0.08	0.07	13.67	13.15	13.32	1.81	0.13	0.92
sum	100.90	100.94	100.09	101.12	99.66	100.35	100.86	99.82	100.57	100.67	100.74	99.99	100.09	99.61	99.53	99.44	99.23
Si	2.940	2.943	2.962	2.816	2.800	2.809	2.951	2.946	2.817	2.792	2.804	2.943	2.923	2.937	2.836	2.799	2.810
Al	1.061	1.059	1.043	1.192	1.201	1.196	1.048	1.057	1.190	1.214	1.201	1.055	1.073	1.059	1.151	1.191	1.178
Fe	0.004	0.003	0.006	0.006	0.000	0.004	0.005	0.074	0.002	0.002	0.002	0.002	0.001	0.004	0.001	0.002	0.004
Ca	0.023	0.004	0.003	0.191	0.209	0.193	0.006	0.005	0.149	0.196	0.184	0.003	0.000	0.000	0.147	0.205	0.188
Sr	0.000	0.000	0.004	0.001	0.000	0.002	0.000	0.002	0.003	0.001	0.001	0.001	0.000	0.000	0.000	0.000	0.000
Ba	0.041	0.055	0.025	0.000	0.000	0.000	0.046	0.052	0.006	0.000	0.000	0.048	0.072	0.064	0.008	0.001	0.001
Na	0.288	0.164	0.138	0.709	0.771	0.784	0.208	0.164	0.652	0.793	0.806	0.145	0.153	0.146	0.786	0.813	0.796
K	0.639	0.772	0.827	0.071	0.010	0.007	0.740	0.768	0.202	0.005	0.004	0.816	0.791	0.803	0.103	0.007	0.053
sum	4.996	4.999	5.009	4.986	4.991	4.995	5.003	5.067	5.020	5.003	5.003	5.013	5.013	5.013	5.034	5.018	5.030
Cn	4.2	5.5	2.5	0.0	0.0	0.0	4.6	5.2	0.6	0.0	0.0	4.7	7.1	6.3	0.8	0.1	0.1
An	2.3	0.4	0.3	19.6	21.1	19.5	0.6	0.5	14.7	19.7	18.5	0.3	0.0	0.0	14.1	20.0	18.1
Sl	0.0	0.4	0.3	0.1	0.0	0.2	0.0	0.2	0.3	0.1	0.1	0.1	0.0	0.0	0.0	0.0	0.0
Ab	29.1	16.5	13.9	72.8	77.8	79.3	20.8	16.5	64.2	79.6	80.8	14.3	15.0	14.4	75.2	79.3	76.7
Or	64.4	77.2	82.6	7.3	1.0	0.7	74.0	77.3	20.0	0.5	0.4	80.5	77.8	79.2	9.9	0.7	5.1

Abbreviations: Ab - albite, An - anorthite, Hy - hyalophane, Kfs - K feldspar, Pg - plagioclase, Or - orthoclase, Sl - slawsonite, Cn - celsian
*Analyst CLC = C.L. Claflin

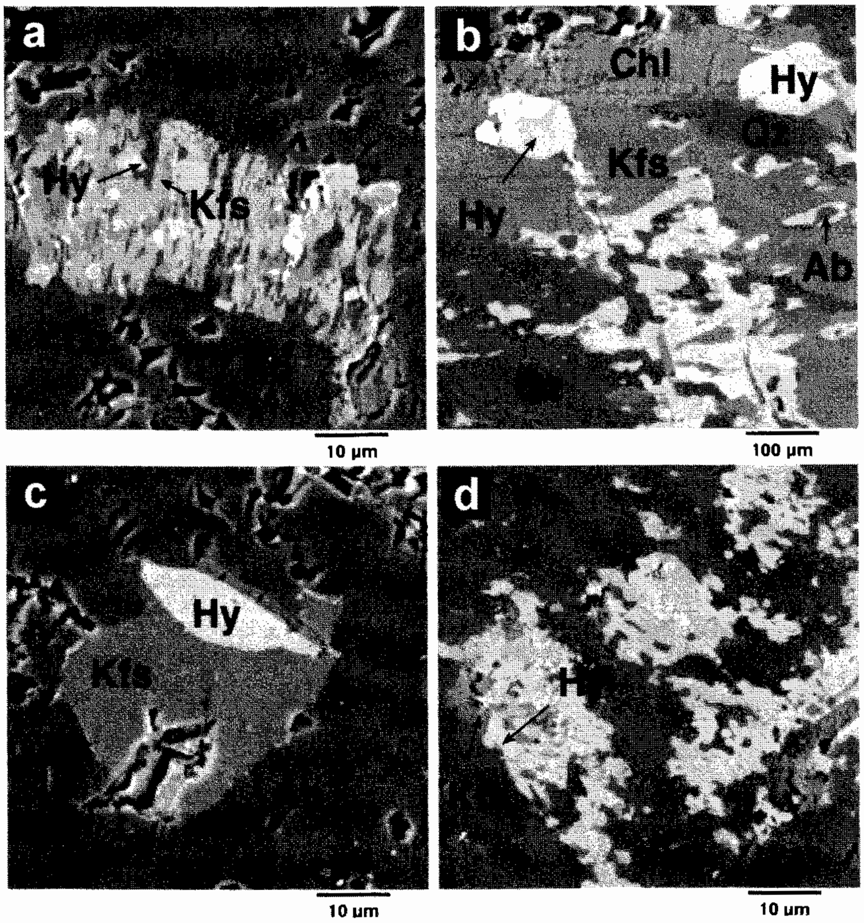

Fig. 1. BSE images of feldspars from the Uppony metasandstone: (a): hyalophane (bright): intergrown with K-feldspar (intermediate grey) in a dark matrix of albite and quartz. Some lamellae of albite extend into the area of K-feldspar and hyalophane. (b): bright "arrowheads" of hyalophane, some with dark cores of albite, surrounded by K-feldspar, in a dark matrix of albite and quartz. (c): bright hyalophane surrounded by homogeneous K-feldspar, in a dark matrix of albite and quartz. (d): fine patchy intergrowth of hyalophane and K-feldspar, too small to analyze by electron microprobe. The textures are not indicative of exsolution but of a complex history. In all these images, the Ba feldspar may have been formed by introduction of Ba-bearing fluids, yet interlocking grains of K-feldspar, albite and hyalophane are also common. Ab = albite, Hy = hyalophane, Kfs = K-feldspar, Qz = quartz, Chl = chlorite.

8 oxygens. Average modes of host and lamellae from homogeneously distributed intergrowths were obtained from BSE images by CLC with the program *NIH Image 1.62* (*http://rsb.info.nih.gov/nih-image/*). Volume percentages were converted to weight percentages using densities of hyalophane (Zaslivskiy *et al.*, 1974) and plagioclase (Carpenter *et al.*, 1985) for compositions similar to the analyzed minerals.

An analytical problem arises for electron microprobe analysis of Ca in barian feldspar in a matrix of calcite, resulting from fluorescence of Ca X-rays in matrix calcite by Ba*L*α X-rays potentially over scales of 10-50 μm. The EMP analysis of Ca in small hyalophane grains or margins of large grains is therefore suspect in marbles. Tests by EJE showed that 1-2 wt % of CaO in hyalophane is produced by matrix fluorescence during analysis of the center of a 10 μm diameter hyalophane with 23 wt % BaO in a calcite host at 15 kV. Analyses of the same grain gave 0.7 wt % CaO at 10 kV and only 0.1 wt % at 6 kV. Therefore, the analyses of EJE on hyalophane and celsian in marble were conducted at 6 kV; the analyses of MAR and CLC, and of EJE on the Hungarian samples, were obtained at 15 kV. Most of the Ca in the celsian analyses of MAR (Table 4) is probably produced by matrix fluorescence. All analyses were conducted at 10 nA beam current with a rastered 3x3 μm beam. Time tests by EJE showed no elemental mobilization under these conditions.

Transmission electron microscope (TEM) studies were undertaken by GG and PMM with samples of the rock chips from the Uppony sandstone. They were mounted with sticky wax and examined with an SEM to select portions that were ion milled. The ion-milled samples were analyzed with a JEOL 2010 TEM equipped with an energy dispersive microanalytical system (EDS) Link-ISIS and operated at 200 kV. Areas of hyalophane that were thin enough to transmit electrons were examined with the TEM and were tilted to find favorable orientations for selected area diffraction studies. Lattice fringe images were examined across the boundaries between hyalophane and both K-feldspar and albite. Analytical electron microscopy (AEM) was undertaken on hyalophane although results are regarded as only qualitative.

Textural observations and analytical results

BSE images reveal textures of coexisting feldspars and show that hyalophane is often chemically heterogeneous. The assemblage hyalophane–albite–microcline occurs in the Uppony sample. The textures are highly variable, some suggesting erratic replacement of an original feldspar clast (Fig. 1a), others showing albite cores and hyalophane rims (Fig. 1b), subhedral hyalophane and microcline in a quartz–albite matrix (Fig. 1b, 1c), and complex textures with interlocking hyalophane, albite and microcline (Fig. 1d). The composition of the Uppony hyalophane varies somewhat from $Cn_{24}Ab_7Or_{69}$ to $Cn_{34}Ab_5Or_{61}$, the albite is $Ab_{99\text{-}100}$ and the microcline is $Cn_{3\text{-}4}Ab_{3\text{-}4}Or_{93}$ (Table 2).

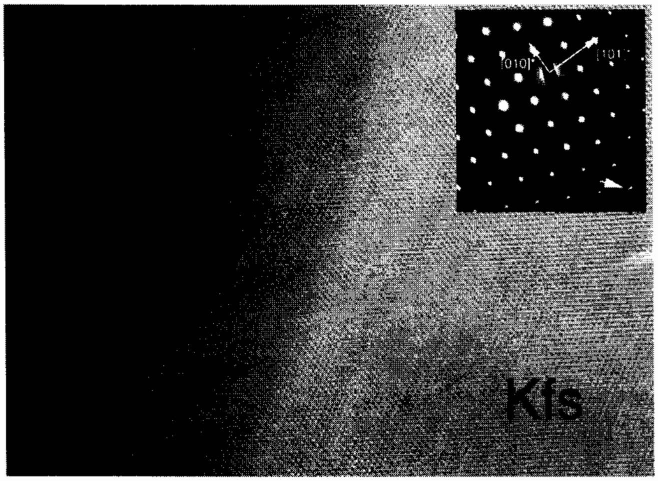

Fig. 2. High resolution image across the hyalophane (Hy)–K-feldspar (Kfs) contact. Lattice fringes are continuous and no spacing change can be detected across the contact. Inset: corresponding selected area diffraction pattern along [101]. Although difficult to detect in figure, reflections are split as illustrated by the thicker arrow. The two thin arrows indicate the [010]* and [-201]* reflections.

Transmission electron microscope (TEM) observations on the boundary between two feldspars in the Uppony samples show coherency between adjacent K-feldspar and hyalophane, and incoherency between albite and hyalophane. No submicroscopic exsolution lamellae were observed with the TEM. Figure 2 shows a high-resolution image of the contact between K-feldspar (lighter area) and hyalophane (darker area). The two sets of lattice fringes are continuous across the contact, and no significant change in their spacing is seen at the boundary. This indicates that the K-feldspar and hyalophane are coherently or at least semi-coherently intergrown at the nm scale. The selected area diffraction pattern (inset in Fig. 2) confirms that the two crystals have the same structure. Reflections with smaller d-values are split along a direction perpendicular to b*, indicating that the two phases have slightly different orientations. Qualitative chemical analyses on K-feldspar and hyalophane grains show that the K-feldspar does not contain any Ba at the *ca.* 0.1-0.2 wt % detection limit of AEM analysis, the hyalophane has no detectable Na, and that its Ba/K ratio does not change towards the contact with K-feldspar.

Barian feldspars from the Grenville marbles are chemically variable from grain to grain and may show complex zoning patterns in BSE images. Sample KA901B from Madoc (Table 3) has hyalophane varying from $Cn_{22}An_3Ab_{13}Or_{62}$ to $Cn_{38}An_2Ab_8Or_{52}$. Some of the hyalophane porphyroblasts are zoned, including one varying from $Cn_{25}An_2Ab_{11}Or_{62}$ to $Cn_{30}An_2Ab_7Or_{60}$. One analyzed hyalophane ($Cn_{30}An_2Ab_7Or_{60}$) is located nearby porphyroblasts of albite (An_7Ab_{93}) and microcline ($Cn_5Ab_9Or_{86}$). The second sample KA914A from Madoc has domains of celsian ($Cn_{93}An_3Ab_2Or_2$) with nearby albite (Ab_{100}) (Table 4). Some celsian is replaced or overgrown with rims of K-feldspar ($Cn_4An_2Ab_1Or_{93}$). Sample BA904A from near Bancroft (Fig. 3a) has discontinuous zones of $Cn_{6\text{-}10}$ (intermediate grey) and Cn_{14} (bright rims), all with a nearly constant albite content (Table 5). Similar zoning and patchy

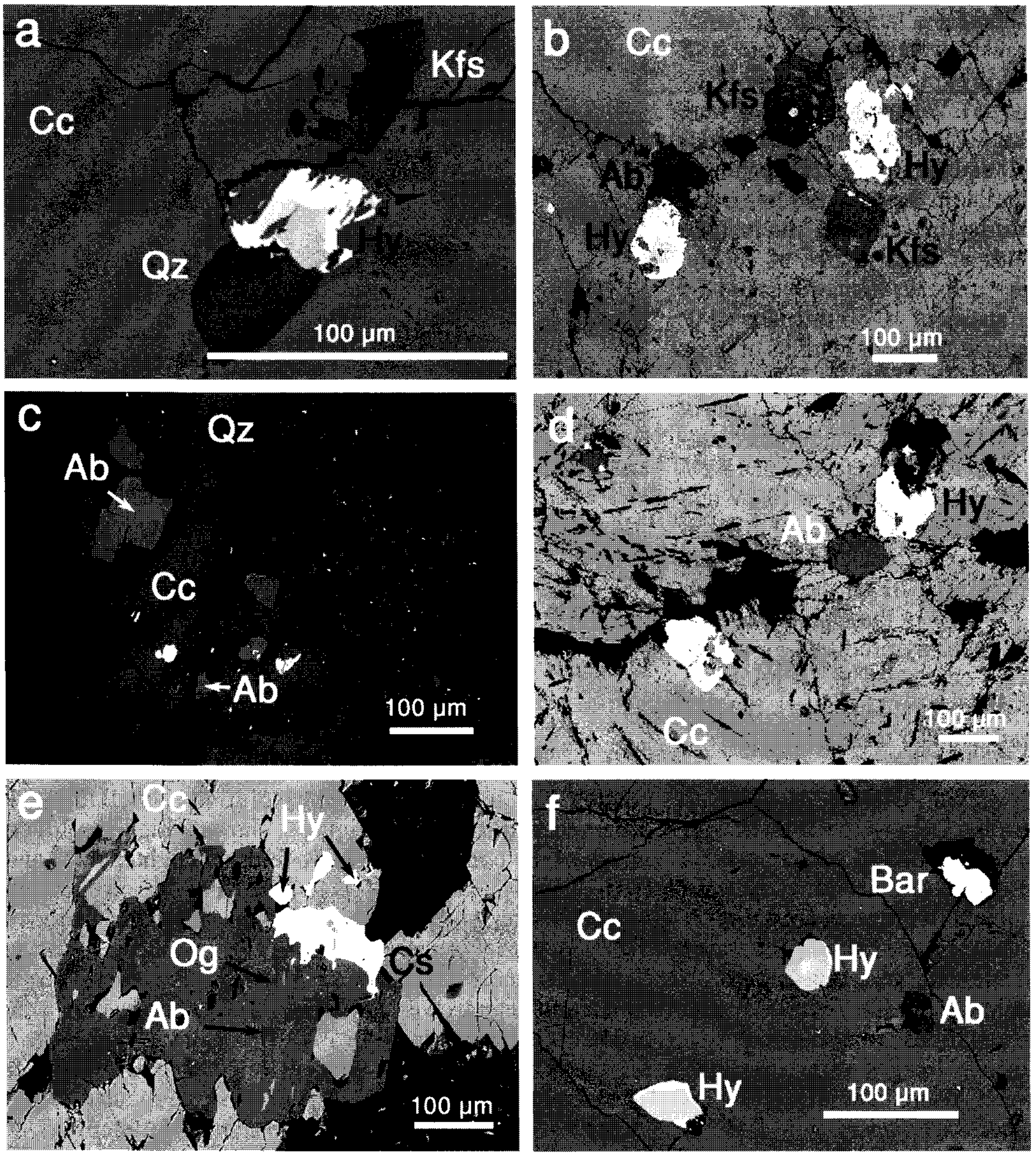

Fig. 3. BSE images of Grenville feldspar porphyroblasts from barian marbles: (a): discontinuously zoned hyalophane in BA901B with a core of Cn_6 and rim of Cn_{14} with nearby albite and quartz; (b): equant grains of celsian and nearby albite in KA914A; (c): celsian replaced by Ba-free K-feldspar in KA914A. (d): grains of albite and hyalophane in calcite (KA901B); (e): albite with inclusions of celsian (K901B); (f) albite with overgrowths of celsian and nearby hyalophane in matrix calcite (KA914A). Albite (darker areas) forms complex intergrowths with oligoclase (lighter areas). Abbreviations: Ab = albite, Bar = barite, Cc = calcite, Cn = celsian, Hy = hyalophane, Kfs = K-feldspar, Og = oligoclase, Qz = quartz.

variation in the Ba content of other hyalophane grains is seen in Fig. 3b and 3f. The textures and the small changes in composition suggest that each zone grew at somewhat different times. The barian feldspars have different compositional ranges in each Grenville marble: Cn_{4-14} (KA904A), Cn_{23-38} (KA901B), Cn_{22-44} (BB9224), and Cn_{81-86} (KA914A). When present, the coexisting plagioclase is usually albite: Ab_{99} (KA901B), Ab_{100} (KA914B) and Ab_{99} (KA914A). An intergrowth of albite (Ab_{99}) with oligoclase (Ab_{78}) is faintly discernable in BSE in sample (Fig. 3e). This assemblage seems to represent the peristerite solvus, but it is unclear whether it equilibrated at the peak of metamorphism or with adjacent hyalophane porphyroblasts. In KA914A, some of the albite grains have nearby grains (Fig. 3c) or rims (Fig. 3e) of celsian. Obvious disequilibrium assemblages are also found in the same rock. Some microcline that rims celsian has very low Na and Ba, implying that it did not equilibrate with albite, celsian or hyalophane. Patchy oligoclase is intergrown with some of the albite, and some is rimmed by homogeneous celsian with nearby hyalophane (Fig. 3e). A single grain of sodic celsian was found as an inclusion in an albite grain in sample BB9224. It is interpreted to be in local equilibrium with the host albite only.

The Wisconsin monzonite originally contained two ternary feldspars: alkali feldspar and sodic plagioclase. The alkali feldspar decomposed forming spectacular symplectic intergrowths (Fig. 4a, 4b, 4c) of barian microcline ($Or_{75-80}Cn_{8-11}Ab_{8-13}An_2$) and oligoclase ($Ab_{79}An_{18}Or_2Cn_1$), with outer rims (Fig. 4c) of microcline ($Or_{75}Ab_{22}Cn_2An_1$) and albite. The plagioclase unmixed to an oligoclase host ($Ab_{78}An_{21}Or_{0.8}Cn_{0.2}$) with antiperthitic lamellae (Fig. 4d) of barian microcline ($Or_{79}Ab_{13}\,Cn_7An_1$). Reintegration of the now exsolved alkali feldspar yields a core of $Ab_{46}Or_{42}An_9Cn_3$ and a rim of $Ab_{46}Or_{44}An_9Cn_1$. The plagioclase host with sparse antiperthite lamellae unmixed from an original composition of $Ab_{69}An_{18}Or_{12}Cn_1$. Although the reintegrated sanidine is too calcic to have

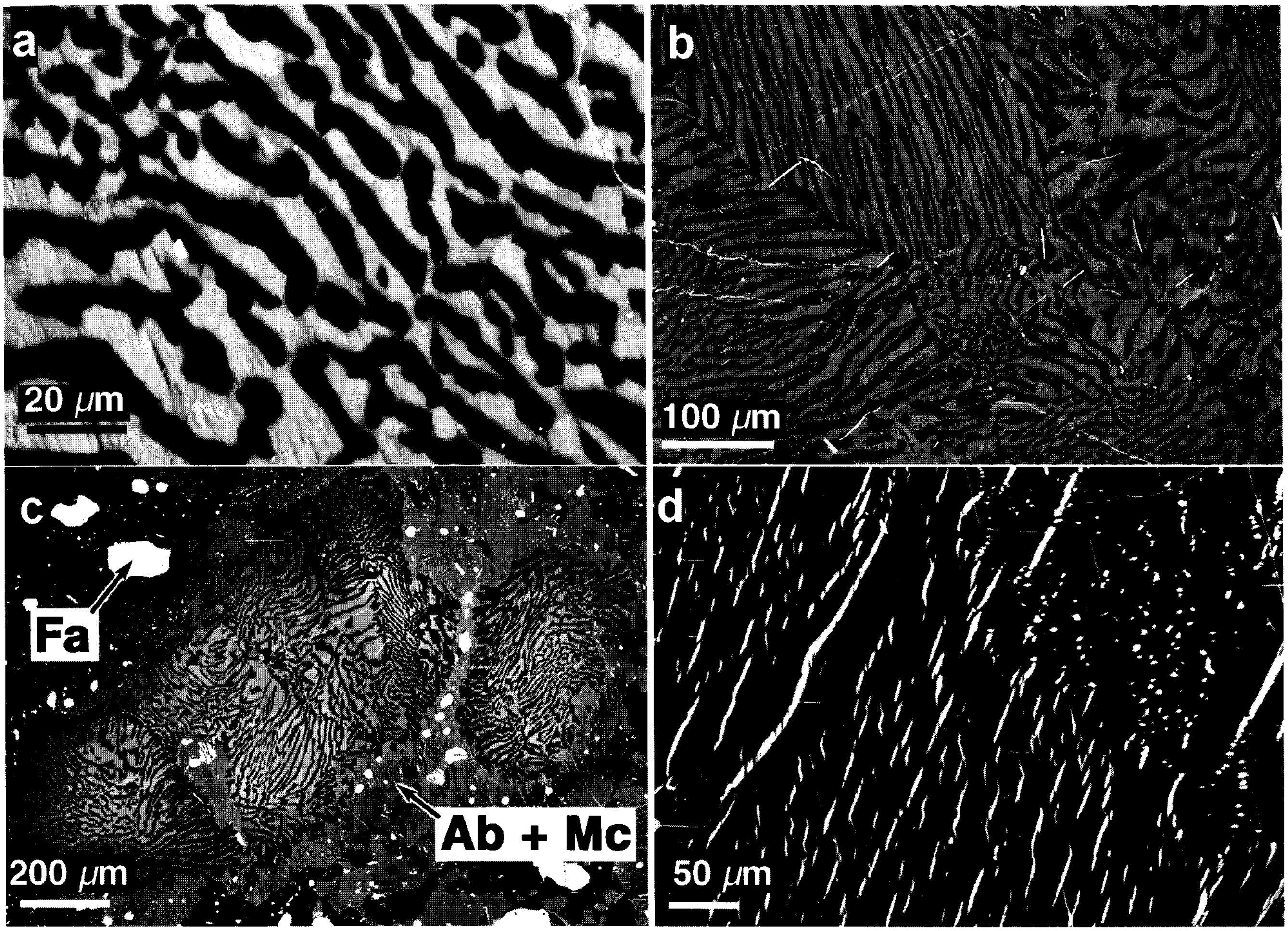

Fig. 4. BSE images of exsolved hyalophane and plagioclase from the Peshtigo monzonite: (a): symplectic intergrowth of K-feldspar (gray): and albite (dark); (b): lower magnification view of symplectic exsolution texture; (c): two symplectic grains with surrounding rim comprised of fine, flame-like intergrowths of microcline and albite. The contrast decreases in hyalophane (gray) toward the rims of the grains due to its gradual depletion in Ba. The dark matrix is quartz and albite, the large bright grains are fayalite overgrowing and replacing ferrosilite, and the smaller bright grains are ilmenite and magnetite. (d): antiperthite with oligoclase (light gray) and microcline lamellae (brighter rods and laths).

equilibrated with the reintegrated plagioclase, application of limiting feldspar thermometry gives 820-870°C at 2 kbar with the program Solvcalc (Wen & Nekvasil, 1994) whereas 450-520°C is obtained for the exsolved host and lamella pairs. The original igneous anorthoclase and oligoclase formed above the solidus and reequilibrated by exsolution in the subsolidus during cooling of the monzonite intrusion.

Discussion

Miscibility gaps with Ba-feldspars

Hyalophane–celsian assemblages

A solvus gap between celsian and hyalophane is well documented by observations of natural assemblages. Viswanathan (1978) identified submicroscopic intergrowths of celsian ($Cn_{99}Or_1$) and hyalophane ($Cn_{46}Or_{54}$) in samples from manganese-rich rocks from Otjosondu, Namibia. Viswanathan & Kielhorn (1983a) reported a coarse interlocking two-phase assemblage from Otjosondu involving hyalophane ($Cn_{51}Ab_{32}Or_{36}$) and celsian ($Cn_{95}Or_5$) that was metamorphosed in the upper amphibolite facies. They also identified exsolution lamellae of celsian ($Cn_{95}Or_5$) in hyalophane ($Cn_{53}Ab_{12}Or_{35}$). The lamellae are sufficiently small (≤ 1 μm) that direct electron microprobe analyses could not be obtained. Pan & Fleet (1991) described hyalophane ($Cn_{47}Ab_{12}Or_{41}$) rimmed by celsian ($Cn_{96}Ab_1Or_3$) in middle amphibolite facies rocks. Kribek *et al.* (1996) found no large discontinuity in compositions between celsian (Cn_{97}) and hyalophane (Cn_{55}) from sediments metamorphosed in the upper amphibolite facies. Devaraju *et al.* (1999) found a jump from $Cn_{91}Ab_2Or_7$ to $Cn_{70}Ab_5Or_{25}$ in a zoned feldspar from rocks that were metamorphosed in the mid-amphibolite facies at Ghattihosahalli, India (Deer *et al.*, 2001, Fig. 579, p. 919).

If the discontinuity is related to a solvus between celsian and hyalophane, it suggests a narrower miscibility gap than at Otjosondo (Viswanathan & Kielhorn, 1983a).

Hyalophane–albite and celsian–albite assemblages

Limited miscibility between albite and hyalophane is well established in low- to medium-grade metamorphic rocks. Nakano (1977, 1979) found hyalophane ($Cn_{17}Ab_5Or_{77}$) with patchy to oriented intergrowths of barian orthoclase ($Cn_4Ab_5Or_{91}$) and albite ($Ab_{99}Or_1$). He concluded that orthoclase unmixed from hyalophane across a solvus and that albite later replaced the feldspars. Viswanathan & Kielhorn (1983a) described exsolved albite in sodian hyalophane from Otjosondu, Namibia. Coats *et al.* (1984) found coexisting hyalophane ($Cn_{55}Ab_{14}Or_{31}$) and albite (Ab_{99}) in calcareous schists from lower amphibolite facies rocks of the Dalradian, Scotland. Zebec & Bermanec (1985) identified oriented intergrowths between hyalophane and albite from Bosnia that may represent exsolution from a homogeneous feldspar. Chabu & Boulègue (1992) observed hyalophane with an inclusion of albite that they suggested formed by exsolution. Barian hyalophane may contain 25-35 % Ab in high-grade metamorphic rocks (Bauer & Palache, 1926; de Villiers, 1951; Lahtinen & Johanson, 1987; Viswanathan & Kielhorn, 1983a; Fortey & Beddoe-Stevens, 1982; Chabu & Boulègue, 1992; Devaraju *et al.*, 1999) and up to 70% Ab in some igneous rocks (Goodfellow *et al.*, 1995; Langworthy & Black, 1978; Tsyganov & Vrublevskaya, 1998). The mutual solution between albite and hyalophane is restricted at low temperatures but expands dramatically at high temperatures.

Celsian ($Cn_{96}Ab_1Or_3$) coexisting with albite (Ab_{100}) was found in manganese-rich metacherts from greenschist facies rocks of eastern Taiwan (Yui *et al.*, 1989) and in albitites and omphacitites from Guatemala (Harlow, 1994, 1995). Zak (1991) described celsian ($Cn_{86}Ab_7Or_7$) intergrown with albite in veins from eastern Bohemia. The amount of Ab in celsian coexisting with albite is comparable to that seen in the Madoc black marble in the greenschist facies. An inclusion of sodian celsian ($C_{66}Ab_{21}Or_9$ Sl_2An_1)was also found included in an albite grain in the Coe Hill marble from the sillimanite zone.

Celsian–plagioclase assemblages

Celsian has been found with significant anorthite and also coexisting with plagioclase. Segnit (1946) reported a calcian celsian from high-grade rocks at Broken Hill, Australia. Mason (1987) found that Segnit's "calciocelsian" was an intergrowth of armenite and celsian, although Deer *et al.* (2001, p. 927) criticized that interpretation based on density considerations. Matsubara (1985) found calcian celsian ($Cn_{75}An_{32}Sl_1Ab_1Or_1$) in a low-temperature setting from Sarusaka, Japan. On the other hand, Frank (1979) described Ca-poor celsian ($Cn_{91}An_1Ab_7Or_1$) with plagioclase ($Ab_{57}An_{43}$) and zoisite in Alpine granitic gneisses of the Berisal Complex, Central Alps, Switzerland, which were subjected to mid-amphibolite facies metamorphism. The apparent decrease in the Ca content of celsian coexisting with plagioclase with increasing temperature is unexpected. One of four possibilities may be suggested: (1) celsian coexisting with more sodic plagioclase takes up less Ca; (2) calcian celsian formed metastably from a greatly supersaturated solution at Sarusaka; (3) calcian celsian is actually paracelsian; or (4) the Berisal feldspar compositions were reset by later exchange on cooling or during retrogression to form zoisite.

Hyalophane–plagioclase assemblages

Hyalophane–plagioclase pairs span a miscibility gap in the quaternary feldspar system $BaAl_2Si_2O_8$–$CaAl_2Si_2O_8$–$NaAlSi_3O_8$–$KAlSi_3O_8$. Meier & Tomlinson (1939) found antiperthitic hyalophane with plagioclase in an altered gabbroic dike. Lahtinen & Johanson (1987) analyzed perthitic hyalophane ($Cn_{23}Ab_{23}Or_{54}$) and exsolved plagioclase ($An_{25\text{-}40}$) from a barian phlogopite-sillimanite–cordierite gneiss in granulites near Pukkiharju, central Finland. These data indicate that hyalophane has substantial solution of plagioclase at high T ,and also that the hyalophane-plagioclase solvus is wide at low T with strong partitioning of Ca in the plagioclase. Grew *et al.* (1991) described hyalophane with subordinate plagioclase and serendibite in granulite facies rocks from near Johnsburg in the Adirondacks, NY. Pan & Fleet (1991) reported plagioclase ($An_{37}Sl_1Ab_{62}$) with unanalyzed hyalophane from a regionally metamorphosed barite unit in greenstones with occasional kyanite and staurolite in adjacent metapelites at Hemlo, Ontario. The authors did not show the textures of the two feldspars, and it is unclear whether they equilibrated. Yan *et al.* (1991) found barian K-feldspar ($Cn_{11}Ab_{13}Or_{76}$) with plagioclase ($An_{30}Ab_{69}Or_1$). Korinevsky (2004) analyzed a barian K-feldspar ($Cn_7An_2Ab_{11}Or_{80}$) forming interlocking to intergrown grains with laboradorite ($An_{50\text{-}55}Sl_2Ab_{40\text{-}46}Or_{2\text{-}3}$) in a gabbro from the Urals. Some of the textures are suggestive of exsolution from an original feldspar. Unfortunately, the analytical totals of the feldspars were miscalculated, and those for hyalophane are unacceptable (103.9-104.6 oxide wt. %). Collectively, available data indicate that hyalophane may coexist with plagioclase in metamorphic rocks, that Sr is strongly favored in plagioclase over hyalophane, and *vice-versa* for Ba.

Celsian–slawsonite assemblages

Matsubara (1985) described calcian celsian ($Cn_{76}An_{32}Sl_1Ab_1Or_1$) with slawsonite ($Sl_{96}Cn_3$) and grossular, hydrogrossular, prehnite, vesuvianite, cymrite, chlorite, diopside and xonotlite in a xenolith contained in an ultramafic body from Sarusaka, Japan. It is surprising that slawsonite ($SrAl_2Si_2O_8$) and celsian ($BaAl_2Si_2O_8$) show little mutual miscibility at the presumed low temperatures (*ca.* 300-400°C) of this rodingite-like occurrence. This result is in striking contrast with the continuous solid solution obtained in experiments on the join $BaAl_2Si_2O_8$–$SrAl_2Si_2O_8$ at 700°C and 2 kbar (Lagache, 1999). Celsian may take up greater Sr in its structure when it is low in Ca, and more extensive solid solution is expected for paracelsian and slawsonite.

Fu *et al.* (2003) identified Ba–Ca–Sr–Na aluminosilicates in a decompressed eclogite from the Dabie and Sulu terranes in China. They reported celsian with 12-14% Ab and several intermediate compositions between celsian and slawsonite. The latter minerals may be slawsonite-paracelsian solid solutions rather than feldspars. The authors stated that their samples represent the first report of a miscibility gap for quaternary (Ba, Ca, Sr, Na) feldspars in nature. It is not clear from their BSE images, however, that two feldspars are intergrown in their samples. Cundari (1979) had already described coexisting sanidine ($Cn_{17}An_8Sl_6Ab_{26}Or_{43}$) and plagioclase ($Cn_3An_{40}Sl_8Ab_{42}Or_7$) in Roman volcanic rocks. His feldspars span a miscibility gap in the quinary (Ba, Ca, Sr, Na, K) feldspar system.

Assemblages with banalsite or stronalsite

Banalsite ($BaNa_2Al_4Si_4O_{16}$) and stronalsite ($SrNa_2Al_4Si_4O_{16}$) sometimes have been described as feldspars, but they do not lie on the feldspar composition plane and therefore is not encountered in the phase diagrams of this study. They mainly occur in low T veins that cut xenoliths in serpentinites. Celsian and/or hyalophane occurs with banalsite (Kato *et al.*, 1987; Harlow, 1994), and slawsonite with stronalsite (Hori *et al.*, 1987).

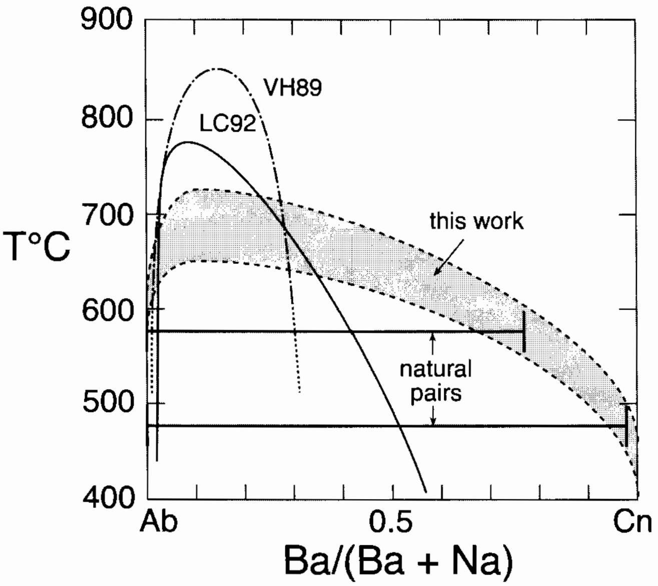

Fig. 5. Phase equilibria in the system $BaAl_2Si_2O_8$–$NaAlSi_3O_8$. Experimental solvi are the dashed (Lagache & Catel, 1992, LC92) and solid lines (Viswnathan & Harneit, 1989, VH89). They are in disagreement with solvus indicated by the compositions of the natural celsian-albite pairs (Yui *et al.*, 1989; this study). Celsian from the upper greenschist facies at 480 ± 20°C has only 2 % Ab, and that from within the sillimanite zone at 575 ± 25°C has 24 % Ab/(Ab+Cn). The inferred solvus (shaded) based on the natural assemblages is much flatter and wider than the experimental solvi.

Experiments on Ba-feldspars

The available experiments on Ba-feldspar joins all involve syntheses rather than reversals. In the system Cn–Or, Roy (1965) obtained continuous solid solution for feldspars synthesized hydrothermally between 500° and 700°C at 2 kbar. Gay & Roy (1968) concluded that disordered hyalophane forms as a solid solution between sanidine and celsian, whereas ordered hyalophane has compositional gaps between Or_{100} and $Cn_{15}Or_{85}$ and between $Cn_{65}Or_{35}$ and $Cn_{80}Or_{20}$. Lagache (1993) undertook exchange experiments in $BaCl_2$ solution with starting materials of $Cn_{25}Or_{75}$ and $Cn_{50}Or_{50}$ that were initially crystallized at 750°C. At 1.5 and 2.3 kbar at 600°C, and at 2.5 kbar and 750°C, she found continuous solid solution between 54 and 94 % Cn.

In experiments on the system Cn–Ab, Viswanathan & Harneit (1989) used synthesis experiments to infer a narrow solvus cresting at 770°C at about $Cn_{15}Ab_{85}$ (Fig. 5, dot-dash line). Lagache & Catel (1992) also conducted experiments on the join at 1-2 kbar with a gel of albite composition or a crystallized albite as a starting material together with aqueous solutions and $BaCl_2$. They inferred a wider and more asymmetrical solvus (Fig. 5, solid line) than Viswanathan & Harneit (1989). Lagache (1993) reported additional exchange experiments on the albite–celsian join with $BaCl_2$ in aqueous solution and provided more experimental detail. She used both gels and crystallized feldspar starting materials, and obtained bulk chemical analyses for Na + Ba on some crystalline run products. At 1.5 kbar and 600°C she converted albite to hyalophane consistent with continuous solid solution between $Cn_{51}Ab_{49}$ and $Cn_{94}Ab_6$. Formation of quartz and barian feldspar in the run products of Lagache & Catel (1992) and Lagache (1993) represents progress of the following reaction to the right:

$$2NaAlSi_3O_8 + BaCl_2\,(Aq) = BaAl_2Si_2O_8 + 2NaCl\,(Aq) + 4SiO_2\,(Qz, Aq) \quad (1).$$

A solvus was inferred when XRD data showed the presence of two feldspars, and their compositions were inferred from powder XRD. An asymmetrical solvus was inferred to crest at Cn_8Ab_{92} and 775°C, Cn_3Ab_{97} coexisting with $Cn_{18}Ab_{82}$ at 750°C, expanding to Cn_8Ab_{92}–$Cn_{40}Ab_{60}$ at 600°C and Cn_2Ab_{98}–$Cn_{53}Ab_{47}$ at 450°C (Fig. 5).

Viswanathan (1992) undertook experiments in the ternary system $BaAl_2Si_2O_8$–$NaAlSi_3O_8$–$KAlSi_3O_8$ using gels as starting material. He inferred a solvus at 650°C based on various untabulated experiments between 650 and 900°C. The inferred limits of the solvus were constructed with the XRD data on run products showing two feldspars as well as experiments yielding one phase. All the experiments with barian feldspars are facing a difficult task in attainment of equilibrium given the very slow diffusion of Ba in feldspars (Cherniak, 2002).

Discussion of experiments

Many of the experiments on phase equilibria relating to barian feldspars were not well documented and no reversals were obtained. Roy's (1965) experiments on Cn–Or may have yielded continuous solutions due to formation of metastably disordered feldspars or as a result of kinetic effects leading to metastable compositions. In the experimental studies of Visnawathan & Harneit (1989) and Lagache & Catel (1992), no run tables were provided with information on the times of experiments, the compositions of starting materials or run products, and the P-T conditions that were used. No run products were analyzed except in a few cases by bulk means. Gels were used as starting materials in many of the experiments, which represent synthesis runs showing only that the crystalline materials are more stable than the starting materials. Homogeneous feldspars were not shown to unmix to two-feldspar assemblages or vice-versa, which is required to document an equilibrium solvus (Essene, 1982, 1989). Reversed experiments should be initiated with wholly crystalline starting materials of highly ordered feldspar to constrain stable solvi involving hyalophane and celsian at 600-800°C. Much longer run times may be required in order to obtain compositional reversals at low P. Experiments could be undertaken with a large volume piston-cylinder at 8-16 kbar in the presence of H_2O while avoiding the stability field of cymrite and K-cymrite.

Celsian–albite pairs from regional metamorphic rocks (Yui *et al.*, 1989; this study) combined with estimates of the estimated peak metamorphic T were plotted in Fig. 5, assuming that the effect of 3-5 kbar on the solvus is small. The Cn-Ab pair at 575 ± 25°C is based on an inclusion of sodian celsian ($Cn_{67}An_1Sl_2Ab_{21}Or_9$) found as an inclusion in albite ($Cn_{0\text{-}1}An_{1\text{-}5}Sl_{0\text{-}1}Ab_{95\text{-}97}Or_0$) in sample BB9224. The celsian is projected onto the diagram assuming that 11 % additional components will not greatly perturb the binary solvus. The natural data indicate a much wider and flatter solvus (shaded area on Fig. 5). More celsian–albite pairs are needed in medium- to high-grade rocks in order to map the locus of the solvus more accurately at higher T. However, the striking disagreement between the natural pairs and experimental curves indicates that the experimental data on the solvus are unreliable.

The experimental data of Lagache & Catel (1992) and Lagache (1993) on the Cn–Ab join show that intermediate feldspars are more stable than the starting material albite + barium chloride solution. Unfortunately, these experiments do not necessarily document stable solvi in the system. Albite in the run products may represent unreacted cores rather than spanning an equilibrium solvus. If so, regrinding and running the sample for longer times with the same fluid should reduce or eliminate the residual albite. The feldspars may contain a vacancy substitution, $\square SiBa_{-1}Al_{-1}$ representing solid solution of $\square_{0.5}Ba_{0.5}AlSi_3O_8$, and equivalent to 50 % $\square Si_4O_8$, which is maximized in the presence of quartz *via* the reaction:

$4SiO_2$ (Qz, Aq) + $BaAl_2Si_2O_8 = 2\ \square_{0.5}Ba_{0.5}AlSi_3O_8$ (2).

In the presence of $BaCl_2$ solution albite may directly react to $\square_{0.5}Ba_{0.5}AlSi_3O_8$ *via*:

$2NaAlSi_3O_8$ + $BaCl_2$ (Aq) = $2\ \square_{0.5}Ba_{0.5}AlSi_3O_8$ + 2NaCl (Aq) (3).

Vacancies therefore may have be involved in the barian feldspars in the experiments of Lagache & Catel (1992) and Lagache (1993).

Skellern *et al.* (2003) serendipitously synthesized single crystals of celsian during reaction of a melt with BaO with an aluminosilicate crucible during slow cooling from 1250°C. They refined its structure and obtained a composition with 40 % $\square_{0.5}Ba_{0.5}AlSi_3O_8$. Their data suggest that celsian formed at very high temperatures may deviate widely from stoichiometry. However, natural celsian forming at metamorphic temperatures (*i.e.*, < 800°C) does not appear to have significant A site deficiencies (Deer *et al.,* 2001). Langworthy & Black (1978) reported analyses of barian anorthoclase and barian sanidine from shonkinites that show systematically low A-site occupancy (0.86-0.93) but lack corresponding excess Si. The apparent A-site deficiency may indicate elemental migration during the analyses or neglect of Sr. Experiments on celsian on the join $BaAl_2Si_2O_8$–SiO_2 show only 1.7 wt% excess SiO_2 (*ca.* 5 mol % $\square_{0.5}Ba_{0.5}AlSi_3O_8$) at 1580°C and less at lower T (Moya Corral & Verduch, 1978). Those data suggest that the vacancy-rich celsian of Skellern *et al.* (2003) is a metastable phase. The experimental barian feldspars (Viswanathan & Harneit, 1989; Lagache & Catel, 1992; Lagache, 1993) nonetheless should be analyzed with the electron microprobe to evaluate whether they have vacancy substitution and compositional heterogeneities. It is a major oversight to rely solely on powder XRD or bulk analytical measurements, as unreacted seeds often persist in subsolidus experiments (*e.g.*, Hayob *et al.*, 1993; Tropper *et al.*, 2002). Experimental runs should be conducted with quartz, ordered celsian and NaCl solution, with low albite, quartz and $BaCl_2$ solution, and with ordered intermediate feldspars on the Cn–Ab join. The run products should also be monitored for any changes in their ordering state, which may influence both the formation and the locus of any solvi (Gay & Roy, 1968).

Compositional gaps in hyalophane solid solutions

Compositional discontinuities within the composition field of hyalophane itself have been inferred repeatedly although their locus and significance remain in dispute. Vermaas (1953) inferred a gap in hyalophane solid solution in the composition range $Cn_{40\text{-}55}$. Gay & Roy (1968) noted discontinuities in the ranges $Cn_{10\text{-}30}$ and $Cn_{60\text{-}80}$, although Chabu & Boulègue (1992) found continuous solid solution in the latter range. Pan & Fleet (1991) placed discontinuities in the ranges $Cn_{15\text{-}25}$, $Cn_{30\text{-}40}$ and $Cn_{65\text{-}96}$, and linked the latter gap to the structural change between hyalophane and celsian. Chabu & Boulègue (1992) found gaps at $Cn_{5\text{-}30}$ and $Cn_{40\text{-}50}$. McSwiggen *et al.* (1994) placed a gap between barian K-feldspar (Cn_9) and hyalophane (Cn_{19}). Their illustrated textures of barian hyalophane in potassian hyalophane are not convincing exsolution features but appear to be irregular veinlets of replacement origin in our opinion, even though the inferred limb of the solvus between microcline and hyalophane is reasonably placed. Bühn *et al.* (1995) found solid solution between K-rich and Ba-rich feldspar up to Cn_{78} in manganese-rich quartzites from granulite facies rocks from Otjosondu, Namibia. Devaraju *et al.* (1999) identified gaps at $Cn_{9\text{-}30}$, $Cn_{40\text{-}58}$, and $Cn_{70\text{-}90}$ in zoned Ba-K feldspars.

The significance of most of the inferred gaps and their widths in the hyalophane series remains unclear. Pan &

Fleet (1991) suggested that the apparent discontinuity at Cn_{30-40} is due to limited sampling, and this may well be the case for most or all of the internal gaps inferred in hyalophane. Plots of electron microprobe analyses of hyalophane show a wide range of compositions with no discontinuities evident in the complete data set except near the join between albite and celsian (Fig. 6). If there were narrow compositional gaps within the composition field of hyalophane that close or migrate laterally with P-T, plots of analytical data from a wide range of P-T such as Fig. 6 would not reveal them. However, inconsistencies in the locations of the internal hyalophane gaps reported at similar metamorphic grades by different authors suggests that they do not represent equilibrium miscibility gaps.

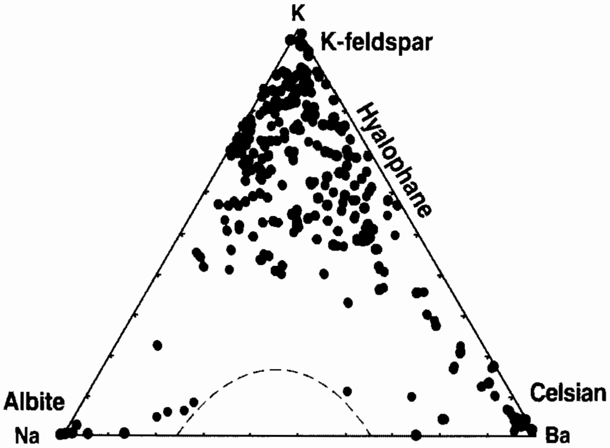

Fig. 6. Analyses of barian feldspars with < 5 mol% $CaAl_2Si_2O_8$, $SrAl_2Si_2O_8$, $KFeSi_3O_8$ in the ternary $BaAl_2Si_2O_8$–$NaAlSi_3O_8$–$KAlSi_3O_8$ (Bauer & Palache, 1926; Nockolds & Zies, 1933, Kalinin, 1939; Meier & Tomlinson, 1939; Yosimura, 1939; Larsen, 1941; Spencer, 1942; Segnit, 1946; de Villiers, 1951; Vermaas, 1953; Novak & Hoffman, 1960; Frondel *et al.*, 1966; Hoffman & Novak, 1966; Boettcher *et al.*, 1967; Wilkinson, 1968; Afonina *et al.*, 1973; Bjørlykke & Griffin, 1973; Klyavin, 1973; Nakamura & Yoder, 1974; Nemec, 1975; Woods, 1976; Nakano, 1977; Langworthy & Black, 1978; Frank, 1979; Marchenko, 1980, 1998; Shramenko *et al.*, 1981; Larsen, 1981, 1982; Reinecke, 1982; Viswanathan & Kielhorn, 1983a; Coats *et al.*, 1984; Cao & Zhou, 1987; Lahtinen & Johnson, 1987; Middlemost *et al.*, 1988; Yui *et al.*, 1989; Jakobsen, 1990; Pivec *et al.*, 1990; Grew *et al.*, 1991; Pan & Fleet, 1991; Yan *et al.*, 1991; Chabu & Boulègue, 1992; Schmädicke *et al.*, 1992; Fortey *et al.*, 1993; Zhang *et al.*, 1993; Harlow, 1994; Long *et al.*, 1994; MCnwiggen *et al.*, 1994; Bühn *et al.*, 1995; Goodfellow *et al.*, 1995; Melcher, 1995; Nkoumbou *et al.*, 1995; Kribek *et al.*, 1996; Melluso *et al.*, 1996; Gaeta, 1998; Tsyganov & Vrublevskaya, 1998; Yanev *et al.*, 1998; Devaraju *et al.*, 1999; Fulignati *et al.*, 2000; Moro *et al.*, 2001; Chakhmouradian & Mitchell, 2002; Riley & Bailey, 2003; this work).

Inferred phase equilibria for the system $BaAl_2Si_2O_8$–$NaAlSi_3O_8$–$KAlSi_3O_8$

The available analytical data on barian feldspars are plotted on a composition diagram for $BaAl_2Si_2O_8$–$NaAlSi_3O_8$–$KAlSi_3O_8$ (Fig. 7). Extensive solid solution occurs in nature, although there is a lack of compositions in the field between albite and celsian, extending into the diagram below the dashed line. Diagrams were constructed separately for diagenetic (Fig. 7a), blueschist and greenschist (Fig. 7c), low to middle amphibolite (Fig. 7d), and upper amphibolite to granulite facies (Fig. 7e). Barian feldspars from igneous (Fig. 8) and vein associations (Fig. 7b) were plotted separately. The Uppony samples contain the three-feldspar assemblage hyalophane–albite–K-feldspar (Fig. 7a). The wide solvus between hyalophane and K-feldspar may indicate that they are not in equilibrium, or that the solvus rapidly expands at low T. The three-phase assemblages from Madoc of hyalophane–microcline–albite and celsian–hyalophane–albite were found in different samples from the same outcrop in the upper greenschist facies. Viswanathan (1992) did not show these three-phase fields in his composition diagram although they are consistent with his data. When found with albite, hyalophane in low-grade rocks has only 5-10 % Ab whereas it may contain 30 % Ab (Bühn *et al.*, 1995) in high-grade rocks. Phase equilibria for $BaAl_2Si_2O_8$–$NaAlSi_3O_8$–$KAlSi_3O_8$ were constructed based on natural assemblages for rocks that metamorphosed in diagenetic conditions at 100-250°C (Fig. 7a), greenschist and blueschist facies (estimated T of 300-500°C; Fig. 7c), low to middle amphibolite facies (estimated T of 500-650°C; Fig. 7d), and upper amphibolite to granulite facies (estimated T of 650-850°C; Fig. 7e). The assumption in applying these crude separations is that T provides the dominant control on solvus locations and that P can be ignored as a first approximation. To the extent that the diagrams are internally consistent and show regular patterns from one to the next is an indication that this assumption is broadly valid.

Ba-feldspars in regionally metamorphosed rocks

Most works on diagenetic feldspars do not include chemical analyses (*e.g.*, Kastner & Siever, 1979; Walker, 1984; Saigal *et al.,* 1988; Lee & Parsons, 2003). Morad *et al.* (1989) analyzed diagenetic K-feldspars but did not obtain data on Ba. Barian feldspar has been reported occasionally in diagenetic environments. Milliken (1989) described authigenic microcline overgrowths on detrital feldspar from the Frio Formation in Texas. Her analytical data are given only in terms of wt% Ba (0-2 wt % Ba, corresponding to *ca.* 0-4 mole % Cn). Bjørlykke & Griffin (1973) identified diagenetic barian feldspars in Ordovician sediments near Oslo, Norway. The hyalophane was easily damaged during analysis by the electron beam. Jakobsen (1990) reported hyalophane ($Ba_{19}Na_2K_{47}$) in black organic chert from North Greenland. The very low A-site total (0.68) of the analysis may be due to sample damage, unanalyzed Sr or NH_4 (Beran *et al.*, 1992), or even vacancy substitution. Moro *et al.* (2001) described K-feldspar, hyalophane, celsian and cymrite in a sedex deposit that was estimated to have formed at 1-2 kbar and 350°C. It is not clear whether the feldspars equilibrated during ore formation, diagenesis or low-grade metamorphism; their analyses were included with the diagenetic samples in this

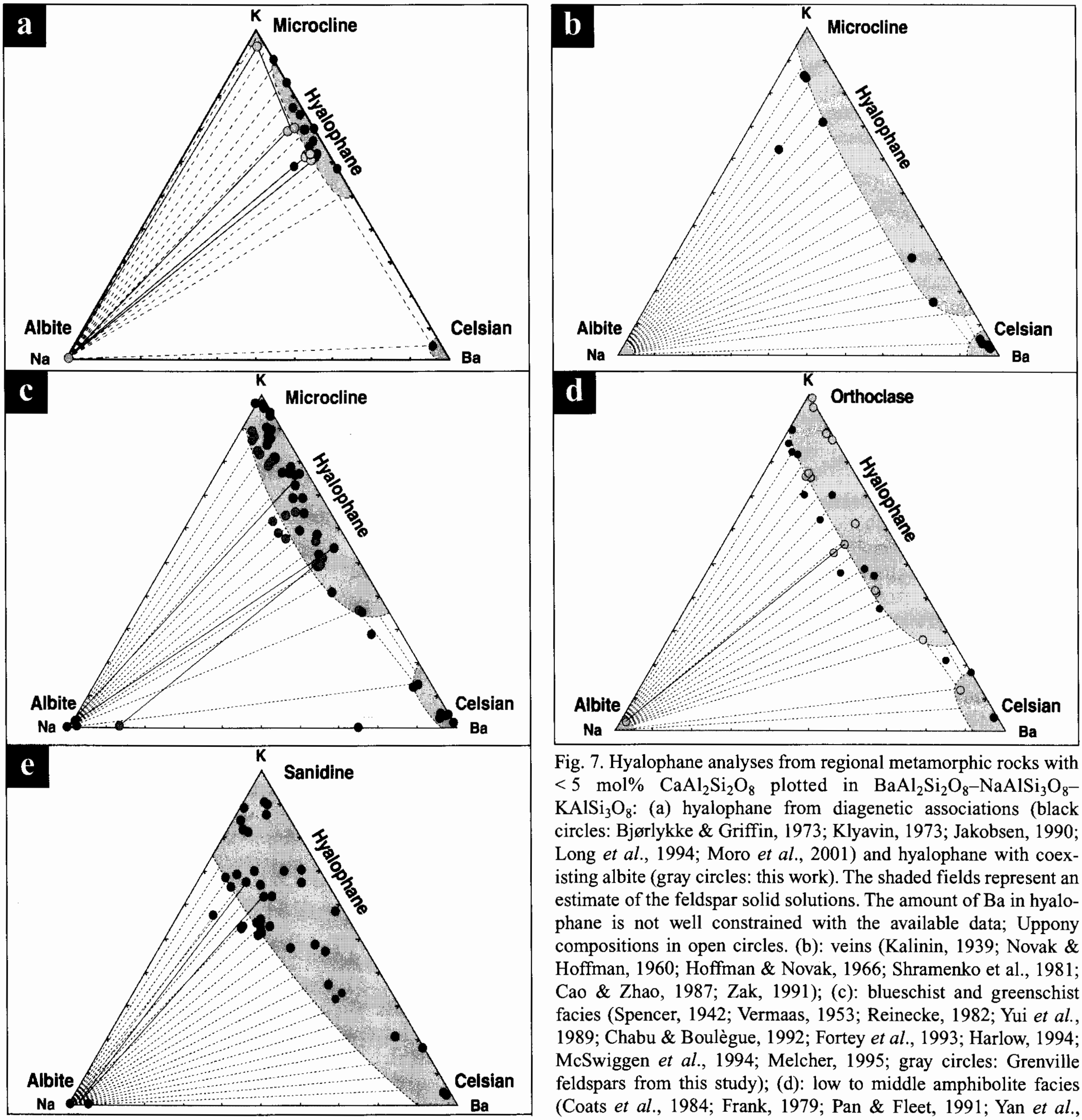

Fig. 7. Hyalophane analyses from regional metamorphic rocks with < 5 mol% $CaAl_2Si_2O_8$ plotted in $BaAl_2Si_2O_8$–$NaAlSi_3O_8$–$KAlSi_3O_8$: (a) hyalophane from diagenetic associations (black circles: Bjørlykke & Griffin, 1973; Klyavin, 1973; Jakobsen, 1990; Long *et al.*, 1994; Moro *et al.*, 2001) and hyalophane with coexisting albite (gray circles: this work). The shaded fields represent an estimate of the feldspar solid solutions. The amount of Ba in hyalophane is not well constrained with the available data; Uppony compositions in open circles. (b): veins (Kalinin, 1939; Novak & Hoffman, 1960; Hoffman & Novak, 1966; Shramenko et al., 1981; Cao & Zhao, 1987; Zak, 1991); (c): blueschist and greenschist facies (Spencer, 1942; Vermaas, 1953; Reinecke, 1982; Yui *et al.*, 1989; Chabu & Boulègue, 1992; Fortey *et al.*, 1993; Harlow, 1994; McSwiggen *et al.*, 1994; Melcher, 1995; gray circles: Grenville feldspars from this study); (d): low to middle amphibolite facies (Coats *et al.*, 1984; Frank, 1979; Pan & Fleet, 1991; Yan *et al.*, 1991; Devaraju *et al.*, 1999; gray circles: Grenville feldspars from this study); (e): upper amphibolite to granulite facies (Spencer, 1942; Segnit, 1946; de Villiers, 1951; Vermaas, 1953; Reinecke, 1982; Yui *et al.*, 1989; Grew *et al.*, 1991; Chabu & Boulegue, 1992; Harlow, 1994; McSwiggen *et al.*, 1994; Bühn *et al.*, 1995; Melcher, 1995; Kribek *et al.*, 1996). The shaded areas represent an estimate of the amount of solid solution in the feldspars at different metamorphic grades.

study. At diagenetic conditions, only a few mole % Ba substitutes in K-feldspar and hyalophane is nearly restricted to the join $BaAl_2Si_2O_8$–$KAlSi_3O_8$. The gap between hyalophane and celsian is not well constrained at diagenetic conditions. The exsolution lamellae of hyalophane ($Cn_{53}Ab_{12}Or_{35}$) in celsian ($Cn_{95}Or_5$) described by Viswanathan & Harneit (1989) suggest that the hyalophane–celsian gap is wide at low T. The available data on diagenetic feldspars are plotted in Fig. 7a.

Hyalophane extends from $Cn_{15}Or_{85}$ to $Cn_{50}Or_{50}$ with very limited Na substitution in the greenschist and blueschist facies (Fig. 7c). It has somewhat more Cn and Ab solution in the lower to middle amphibolite facies (Fig. 7d). In the upper amphibolite facies (Fig. 7e), some workers reported a gap between hyalophane and celsian

(Viswanathan & Kielhorn, 1983a; Viswanathan, 1992), whereas others suggested that the gap is closed (Kribek *et al.*, 1996). Hyalophane and celsian in this facies may both take up more Na and Ca. Continuous solid solution is expected from K-feldspar to celsian in the granulite facies. Hyalophane and celsian may be found with high Ca and often coexisting with plagioclase in higher-grade metamorphic rocks.

Igneous Ba-feldspars

Intrusive and extrusive alkaline igneous rocks may contain barian feldspars. Hyalophane and barian sanidine have been reported in analcitites and phonolites from the Highwood Mountains, Montana (Larsen, 1941; Wilkinson, 1968; Nakamura & Yoder, 1974; Woods, 1976) and the Rainy Creek complex (Boettcher *et al.*, 1967). Barian K-feldspars have also been found in pegmatites (Afonina *et al.*, 1973; Marchenko, 1980; Pivic *et al.*, 1990; Chakhmouradian & Mitchell, 2002) and granites (Nemec, 1975; Yanev *et al.*, 1998). Barian feldspars have been described in a monchiquite of West Greenland (Larsen, 1981), and in a nephelinite from Cameroon (Nkoumbou *et al.*, 1995). Barian sanidine, anorthoclase and plagioclase occur in shonkinites and syenites from central Australia (Langworthy & Black, 1978) and in leuctitites and related alkaline volcanic rocks (Cundari, 1979; Zhang *et al.*, 1993; Gaeta, 1998; Fulignati *et al.*, 2000). Compositional data on barian feldspars from igneous rocks are plotted in Fig. 8. The analyses of the exsolved alkali feldspars from the Peshtigo monzonite of Wisconsin are projected onto two ternary plots in Fig. 9. The Ab and An of the anorthoclase unmixed to yield oligoclase in a microcline host.

Vein Ba-feldspars

In addition to occurrences in igneous and metamorphic rocks, hyalophane is occasionally found in veins. As with adularia, it is possible that vein hyalophane is metastably and variably disordered, and compositions may form that lie within stable solvi. However, most of the sparse compositional data on vein hyalophane (Fig. 7b) is consistent with those in other low temperature occurrences (Fig. 7c).

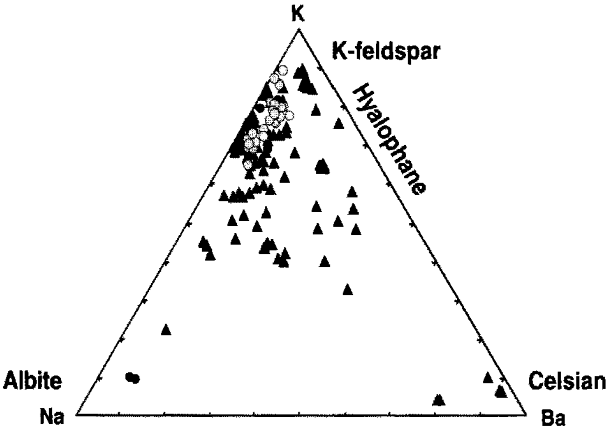

Fig. 8. Igneous hyalophane with < 5 mol% $CaAl_2Si_2O_8$, $SrAl_2Si_2O_8$, $KFeSi_3O_8$ plotted in $BaAl_2Si_2O_8$–$NaAlSi_3O_8$–$KAlSi_3O_8$ (black triangles from Nockolds & Zies, 1933, Meier & Tomlinson, 1939; Larsen, 1941; Boettcher *et al.*, 1967; Wilkinson, 1968; Afonina *et al.*, 1973; Nakamura & Yoder, 1974; Nemec, 1975; Woods, 1976; Langworthy & Black, 1978; Marchenko, 1980, 1998; Larsen, 1981; Middlemost *et al.*, 1988; Pivec *et al.*, 1990; Zhang *et al.*, 1993; Goodfellow *et al.*, 1995; Nkoumbou *et al.*, 1995; Gaeta, 1998; Tsyganov & Vrublevskaya, 1998; Yanev *et al.*, 1998; Fulignati *et al.*, 2000; Chakhmouradian & Mitchell, 2002; Riley & Bailey, 2003). Barian microcline from the Peshtigo monzonite are gray circles (this work).

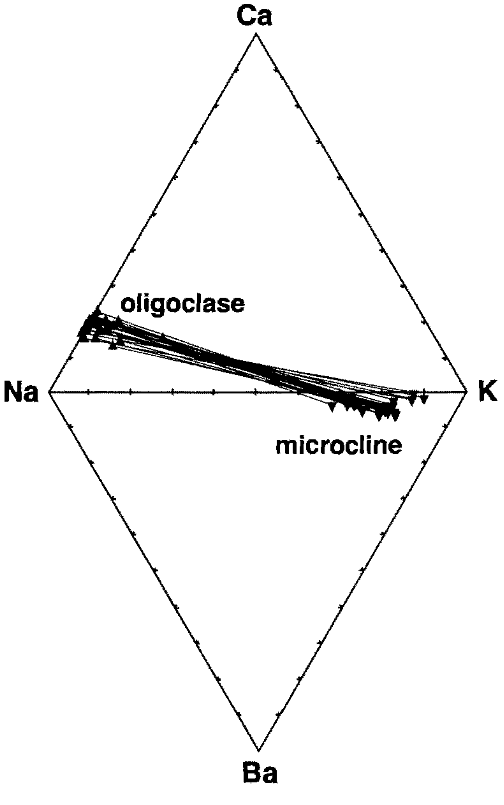

Fig. 9. Compositions of exsolved K-feldspar and albite from the Peshtigo monzonite projected onto $CaAl_2Si_2O_8$–$NaAlSi_3O_8$–$KAlSi_3O_8$ and $BaAl_2Si_2O_8$–$NaAlSi_3O_8$–$KAlSi_3O_8$. The tie-lines drawn between the two composition triangles pass through quaternary composition space.

Na in Ba-feldspars as a geothermometer

Once calibrated the albite content of hyalophane and celsian buffered with albite could be useful as a thermometer. The amount of Na in hyalophane progressively increases with metamorphic grade when buffered in the presence of albite. In diagenetic associations, hyalophane has 3-7 % Ab (Fig. 7a). In the blueschist and greenschist facies, hyalophane takes up 7-11 % Ab in the presence of albite (Fig. 7c), and 14-18 % in the low- to mid-amphibolite facies (Fig. 7d). Hyalophane in the upper amphibolite to granulite facies may have 30 % Ab (Fig. 7e) even when unbuffered with a separate albite phase. The amount of Na in hyalophane and celsian increases rapidly in the T range between 500 and 700°C. If the solvus that has been estimated for celsian-albite is correct, it will also provide a thermometer. Celsian with 12-14 % Ab in a decompressed eclogite (Fu *et al.*, 2003) would require a minimum T of *ca.* 500-550°C if formed in equilibrium at relatively low P (3-6 kbar). The pressure effect on the solvus remains to be evaluated.

Three- and four-feldspar assemblages

Based on direct observation, albite–hyalophane–celsian and albite–microcline–hyalophane are stable in $BaAl_2Si_2O_8$–$NaAlSi_3O_8$–$KAlSi_3O_8$ at low to medium T. Phase equilibria inferred for this system from natural assemblages in this study contrast considerably from experimental diagrams, showing much more restricted substitution of albite in hyalophane and celsian. The width of the two- and three-phase fields may depend in part on the ordering state of the feldspars. Just as in the plagioclase system, ordering of intermediate compositions may perturb solvus widths and perhaps induce low temperature solvi. Growth and persistence of disordered feldspars may affect the development and position of solvi in these systems. Strong evidence for solvi must reside in finding coexisting and/or exsolved assemblages in nature. Although exsolution of hyalophane and celsian has been observed (Viswanathan 1978; Viswanathan & Harneit, 1989), the host and lamellae compositions were not measured directly. Viswanathan & Harneit (1989) also described coarse, interlocking celsian and hyalophane, so the solvus between hyalophane and celsian has been persuasively established.

Other assemblages with both three and four coexisting feldspars may be stable under certain conditions. Two feldspars spanning the peristerite gap between albite and oligoclase occur in the upper greenschist facies (Crawford, 1966; Maruyama *et al.*, 1982). The solvus between albite and microcline is wide, and the assemblage oligoclase–albite–microcline is therefore expected at these conditions in the system $CaAl_2Si_2O_8$–$NaAlSi_3O_8$–$KAlSi_3O_8$. Given the solvus between microcline and hyalophane, hyalophane–oligoclase–albite–microcline should therefore also be stable. This assemblage was found in one Madoc marble, but it is unclear whether the intergrown albite and oligoclase both equilibrated with hyalophane and microcline. The average composition of the unmixed feldspars in the Peshtigo monzonite is close to that expected for a four-feldspar assemblage, where albite was not found with oligoclase, although it is found on the rims with microcline (Fig. 4c). Each four-feldspar assemblage should be bounded by four three-feldspar assemblages (Table 8). The Bøggild and Hüttenlocher solvi in plagioclases may extend up to medium to high T (Smith, 1983). Wenk & Wenk (1984) and Wenk *et al.* (1991) found evidence for these plagioclase gaps in marbles from the amphibolite facies in the Central Alps. They described coexisting plagioclases and a paucity of plagioclase compositions in the region of the gaps. In addition, Wenk *et al.* (1991) also identified an unnamed narrow gap between calcian oligoclase and andesine. Wenk *et al.* (1986) reported three-phase assemblages for K-feldspar and two plagioclases in their marbles. If these plagioclase gaps persist up to moderate T (500-600°C), as many as 8 four-feldspar and 24 three-feldspar assemblages may be stable in $BaAl_2Si_2O_8$–$CaAl_2Si_2O_8$–$NaAlSi_3O_8$– $KAlSi_3O_8$ (Table 6). To the authors' knowledge it has not been suggested previously that four feldspars have a stability field. The three- and four-feldspar gaps will disappear at high T with closure of the solvi. If the phase diagram of Smith (1983) is correct, most plagioclase gaps also disappear at low T and many of the three- and four-phase assemblages would also then vanish.

Even more complex relationships must be anticipated among feldspars and borosilicates. Wide miscibility gaps have been observed for pekovite–reedmergnerite ($NaBSi_3O_8$ feldspar) and meleevite–danburite (Pautov *et al.*, 2004). These data suggest that many multiphase assemblages will occur among borosilicates and aluminosilicates with feldspar and danburite structures. Applying Goldschmidt's phase rule, up to 10 phases might coexist at low to medium T for certain compositional ranges in $BaAl_2Si_2O_8$–$CaAl_2Si_2O_8$–$SrAl_2Si_2O_8$–$NaAlSi_3O_8$–$KAlSi_3O_8$–$BaB_2Si_2O_8$–$CaB_2Si_2O_8$–$SrB_2Si_2O_8$–$NaBSi_3O_8$–$KBSi_3O_8$.

In contrast, the occurrence of low-temperature solvi within the composition field for hyalophane in the range $Cn_{15}Or_{85}$ to $Cn_{55}Or_{45}$ remains uncertain. Gaps in compositional plots permit but do not require a solvus. Compositional jumps in zoned hyalophane may register a change in the composition of the metamorphic fluid during growth rather than indicating a miscibility gap. Disagreement in the position of internal hyalophane discontinuities in different associations is to be expected if variable environmental factors rather than solvi are controlling the composition of Ba-K feldspar during growth over time. Only when interlocking grains of two compositions are found, as well as mutual exsolution of each phase in the other, as has been described for hyalophane–celsian, is a solvus well established. Cherniak (2002) measured the diffusion rate of Ba in sanidine and plagioclase, and found that it diffused about two orders of magnitude more slowly than Ca. He calculated at 700°C that zoning in Ba over 100 μm would take 10 Ma to diffuse away, and 10 μm wide zones would be flattened in 0.5 Ma. Zoning of Ba in feldspars forming at low to medium metamorphic grades will be preserved nearly indefinitely unless the feldspars are recrystallized. The diffusion of Ba in feldspar may be accelerated in the presence of H_2O fluid, especially at high P and under more reducing conditions for which the amount of H_2 is increased. Based on presently available information, the authors conclude that no internal miscibility gaps exist in the hyalophane composition field between 15 and 55% celsian.

Nomenclature of Ba-feldspars

A miscibility gap between barian microcline (Cn_{3-10}) and potassian hyalophane (Cn_{15-25}), and with barian hyalophane (Cn_{55-75}) and celsian (Cn_{95}), is observed at moderate temperatures in nature. Those gaps support the current use of the name hyalophane for intermediate Ba-K feldspars. The name is justified despite the expected continuous solid solution among celsian, sanidine and albite above 700°C. The nomenclature must also address the names of feldspars

Table 8. Possible three- and four-feldspar assemblages in $BaAl_2Si_2O_8$–$KAlSi_3O_8$–$NaAlSi_3O_8$–$CaAl_2Si_2O_8$

Four-phase assemblages	*bounding three-phase assemblages*	#
A. **albite–oligoclase–K·feldspar*–hyalophane**		
	albite–oligoclase–hyalophane	(1)
	albite–oligoclase–K·feldspar	(2)
	albite–K·feldspar–hyalophane	(3)
	oligoclase–K·feldspar–hyalophane	(4)
B. albite–oligoclase–hyalophane–celsian		
	albite–oligoclase–hyalophane	(1)
	albite–hyalophane–celsian	(5)
	albite–oligoclase–celsian	(6)
	oligoclase–hyalophane–celsian	(7)
C. oligoclase–andesine–K·feldspar*–hyalophane		
	oligoclase–andesine–K·feldspar	(8)
	oligoclase–andesine–hyalophane	(9)
	oligoclase–K·feldspar–hyalophane	(4)
	andesine–K·feldspar*–hyalophane	(10)
D. oligoclase–andesine–hyalophane–celsian		
	oligoclase–andesine–hyalophane	(9)
	oligoclase–andesine–celsian	(11)
	oligoclase–hyalophane–celsian	(7)
	andesine–hyalophane–celsian	(12)
E. laboradorite–bytownite–K·feldspar*–hyalophane		
	laboradorite–K·feldspar–bytownite	(13)
	laboradorite–bytownite–hyalophane	(14)
	laboradorite–K·feldspar–hyalophane	(15)
	bytownite–K·feldspar–hyalophane	(16)
F. laboradorite–bytownite–hyalophane–celsian		
	laboradorite–bytownite–hyalophane	(14)
	laboradorite–bytownite–celsian	(17)
	laboradorite–hyalophane–celsian	(18)
	bytownite–hyalophane–celsian	(19)
G. bytownite–anorthite–K.feldspar*–hyalophane		
	bytownite–anorthite–hyalophane	(20)
	bytownite–anorthite–K·feldspar	(21)
	bytownite–K·feldspar–hyalophane	(16)
	anorthite–K·feldspar–hyalophane	(22)
H. bytownite–anorthite–hyalophane–celsian		
	bytownite–anorthite–hyalophane	(20)
	bytownite–anorthite–celsian	(23)
	bytownite–hyalophane–celsian	(19)
	anorthite–hyalophane–celsian	(24)

*The general term K·feldspar is used because it is not clear which $KAlSi_3O_8$ polymorph would be stable.

Observed assemblages in bold: K·feldspar + two plagioclases (Wenk *et al.*, 1991); hyalophane and celsian-bearing assemblages (this paper).

Eight three-phase assemblages are found under two different four-phase assemblages because they bound both of them. Duplicates are indicated in the last column with the same number.

that lie within these miscibility gaps, as may occur especially in rapidly quenched volcanic rocks. Selecting the midpoint between 55 and 95 mole % Cn, it is recommended that any feldspar with > 15 % and < 75 % Cn be named hyalophane and that those with > 75 % Cn be designated as celsian. This recommendation is similar to that of Deer *et al.* (2001), who separated hyalophane from celsian at 80 % Cn. The occurrence of more than one distinct species within the composition range of hyalophane itself depends on the existence of additional miscibility gaps and/or discontinuous changes in the crystal structure in the hyalophane series. Until those relations are better established it is recommended that any feldspar with dominant Ba or K in the composition range of Cn_{15-75} be simply described as hyalophane. Hyalophane with > 50 % Cn may be referred to as barian, and those with < 25 % Cn as potassian. The qualifier sodian may be applied to hyalophane and celsian when Na exceeds 10 mol % of the A site.

Acknowledgments: The authors are grateful to J.L. Anderson for samples from Wisconsin. C.E. Henderson is thanked for maintaining the electron microbeam equipment at Michigan. This work was supported by NSF EAR grants 87-08276, 88-12764, 95-26596, 96-28196, 97-06349, 99-

11352, Department Scott Turner grants to CLC and MAR, and funds from the W.C. Kelly Collegiate Professorship to EJE. Jürgen Konzett and Achille Blasi are acknowledged for reviews of the manuscript.

References

Afonina, G.G., Makagon, V.M., Shmakin, B.M. (1973): Barium-containing potassium feldspars of muscovite pegmatites. *Izv. Akad. Nauk SSSR, Ser. Geol.*, **7**, 87-94.

Anderson, J.L. (1980): Mineral equilibria and crystallization conditions in the late Precambrian Wolf River rapakivi massif, Wisconsin. *Am. J. Sci.*, **280**, 89-332.

Anderson, J.L., Cullers, R.L., Van Schmus, W. (1980): Anorogenic metaluminous and peraluminous granite plutonism in the mid-Proterozoic of Wisconsin. *Contrib. Mineral. Petrol.*, **74**, 311-328.

Anovitz, L.M. & Essene, E.J. (1987): Phase equilibria in the system $CaCO_3$–$MgCO_3$–$FeCO_3$. *J. Petrol.*, **28**, 389-414.

Árkai, P. (1983): Very low- and low-grade Alpine regional metamorphism of the Paleozoic and Mesozoic formations of the Bükkium, NE-Hungary. *Acta Geol. Hung.*, **26**, 83-101.

Árkai, P., Balogh, K., Dunkl, I. (1995): Timing of low-temperature metamorphism and cooling of the Paleozoic and Mesozoic formations of the Bükkium, innermost Western Carpathians, Hungary. *Geol. Rundsch.*, **84**, 334-344.

Árkai, P., Horváth, Z.A., Tóth M. (1981): Transitional very low- and low-grade regional metamorphism of the Paleozoic formations, Uppony Mountains, NE-Hungary: mineral assemblages, illite-crystallinity, b_0 and vitrinite reflectance data. *Acta Geol. Acad. Sci. Hung.*, **24**, 265-294.

Árkai, P., Mata, M.P., Giorgetti, G., Peacor, D.R., Tóth M. (2000): Comparison of diagenetic and low-grade metamorphic evolution of chlorite in associated metapelites and metabasites: an integrated TEM and XRD study. *J. metamorphic Geol.*, **18**, 531-550.

Bambauer, H.U. & Nager, H.E. (1981): Gitterkonstanten und displazive Transformation synthetischer Erdalkalifeldspaete. I. System $CaAl_2Si_2O_8$–$SrAl_2Si_2O_8$–$BaAl_2Si_2O_8$. *N. Jb. Mineral. Abh.*, **141**, 225-239.

Bauer, L.H. & Palache, C. (1926): Hyalophane from Franklin Furnace, New Jersey. *Am. Mineral.*, **11**, 172-174.

Beran, A., Armstrong, J., Rossman, G.R. (1992): Infrared and electron microprobe analysis of ammonium ions in hyalophane feldspar. *Eur. J. Mineral.*, **4**, 847-850.

Bjørlykke, K.O. & Griffin, W.L. (1973): Barium feldspars in Ordovician sediments, Oslo region, Norway. *J. Sed. Petrol.*, **43**, 461-465.

Boettcher, A.L., Piwinskii, A.J., Knowles, C.R. (1967): Zoned potash feldspars from the Rainy Creek complex near Libby, Montana. *Earth Planet. Sci. Lett.*, **3**, 8-10.

Boundy, T.M., Donohue, C.L., Essene E.J., Mezger, K., Austrheim, H. (2002): Discovery of eclogite-facies carbonate rocks from the Lindås Nappe, Western Norway. *J. metamorphic Geol.*, **20**, 649-667.

Brown, P.E., Essene, E.J., Peacor, D.R. (1981): Phase relations inferred from field data for manganese pyroxenes and pyroxenoids. *Contrib. Mineral. Petrol.*, **74**, 417-425.

Bühn, B., Okrusch, M., Woermann, E., Lehnert, K., Hoernes, S. (1995): Metamorphic evolution of Neoproterozoic manganese formations and their country rocks at Otjosondu, Namibia. *J. Petrol.*, **36**, 463-496.

Cao, E. & Zhou, S. (1987): The mineralogy of copper ores in the celsian-bearing rocks in Wujiapo, Shensi. *Shaanxi Dizhi*, **5**, 44-50.

Carpenter, M.A., McConnell, J.D.C., Navrotsky, A. (1985): Enthalpies of ordering in the plagioclase feldspar solid solution. *Geochim. Cosmochim. Acta*, **49**, 947-966.

Chabu, M. & Boulègue, J. (1992): Barian feldspar and muscovite from the Kipushi Zn-Pb-Cu deposit, Shaba, Zaire. *Can. Mineral.*, **30**, 1143-1152.

Chakhmouradian, A.R. & Mitchell, R.H. (2002): The mineralogy of Ba- and Zr-rich alkaline pegmatites from Gordon Butte, Crazy Mountains (Montana, USA): comparisons between potassic and sodic agpaitic pegmatites. *Contrib. Mineral. Petrol.*, **143**, 93-114.

Cherniak, D.J. (2002): Ba diffusion in feldspar. *Geochim. Cosmochim. Acta*, **66**, 1641-1650.

Chiari, G., Calleri, M., Bruno, E., Ribbe, P.H. (1985): Two independent refinements of the structure of paracelsian, $BaAl_2Si_2O_8$. *Am. Mineral.*, **60**, 111-119.

Claflin, C.L. (2001): Thermobarometry of the Peshtigo Monzonite, Wolf River Batholith, Wisconsin, USA. MSc thesis, Univ. Michigan, 45 p.

Coats, J.S., Fortey, N.J., Gallagher, M.J., Grout, A. (1984): Stratiform barium enrichment in the Dalradian of Scotland. *Econ. Geol.*, **79**, 1585-1595.

Cosca, M.A., Essene, E.J., Kunk, M.J., Sutter, J.F. (1992): Differential unroofing within the Central Metasedimentary Belt, Grenville Orogen, Ontario: constraints from $^{40}Ar/^{39}Ar$ thermochronometry. *Contrib. Mineral. Petrol.*, **110**, 211-225.

Crawford, M.L. (1966): Composition of plagioclase and associated minerals in some schists from Vermont, U.S.A., and South Westland, New Zealand, with inferences about the peristerite solvus. *Contrib. Mineral. Petrol.*, **13**, 269-294.

Cundari, A. (1979): Petrogenesis of leucite-bearing lavas in the Roman volcanic region, Italy. *Contr. Mineral. Petrol.*, **70**, 9-21.

de Villiers, J.E. (1951): The manganese ores of Otjosondu, South-West Africa. *Trans. Geol. Soc. S. Africa*, **54**, 89-98.

Deer, W.A., Howie, R.A., Zussman, J. (2001): Barium feldspars. *in:* "Rock-forming minerals: feldspars", Vol. 4A, 2nd ed., The Geological Society, London, 909-942.

Devaraju, T.C., Raith, M.M., Spiering, B. (1999): Mineralogy of the Archean barite deposit of Ghattihosahalli, Karnataka, India. *Can. Mineral.*, **37**, 603-617.

Essene, E.J. (1982): Geologic thermometry and barometry. *in:* "Characterization of metamorphism through mineral equilibria," J. Ferry, ed., *Rev. Mineral.*, **10**, 153-206.

— (1983): Solid solutions and solvi among metamorphic carbonates with applications to geologic thermobarometry. *in:* "Carbonates: mineralogy and chemistry," R.J. Reeder, ed., *Rev. Mineral.*, **11**, 77-96.

— (1989): The current status of thermobarometry in metamorphic rocks. *in:* "Evolution of metamorphic belts", S.R. Daly, R. Cliff, B.W.D. Yardley, eds., *Geol. Soc. Spec. Paper*, **43**, 1-44.

Fortey, N.J. & Beddoe-Stevens, S.B. (1982): Barium silicates in stratabound Ba-Zn mineralization in the Scottish Dalradian. *Mineral. Mag.*, **46**, 63-72.

Frank, E. (1979): Celsian in leucocratic gneisses of the Berisal-Complex, Central Alps, Switzerland. *Schweiz. Mineral. Petrogr. Mitt.*, **59**, 245-250.

Frondel, C., Ito, J., Hendricks, J.G. (1966): Barium feldspars from Franklin Furnace, New Jersey. *Am. Mineral.*, **51**, 1388-1393.

Fu, B., Touret, J.L.R., Zheng, Y.-F., Jahn, B.-M. (2003): Fluid inclusions in granulites, granulitized eclogites and garnet clinopyroxenites from the Dabie-Sulu terranes, eastern China. *Lithos*, **70**, 293-319.

Fulignati, P., Marianelli, P., Sbrana, A. (2000): Glass-bearing felsic nodules from the crystallizing sidewalls of the 1944 Vesuvius magma chamber. *Mineral. Mag.*, **6**, 481-496.

Gaeta, M. (1998): Petrogenetic implications of Ba-sanidine in the Lionato Tuff (Colli Albani Volcanic district, Central Italy). *Mineral. Mag.*, **62**, 697-702.

Gay, P. & Roy, N.N. (1968): The mineralogy of the potassium-barium feldspar series: III. Subsolidus relationships. *Mineral. Mag.*, **36**, 914-932.

Goodfellow, W.D., Cecile, M.P., Leybourne, M.I. (1995): Geochemistry, petrogenesis, and tectonic setting of lower Paleozoic alkalic and potassic volcanic rocks, northern Canadian Cordilleran Miogeocline. *Can. J. Earth Sci.*, **32**, 1236-1254.

Grew, E.S., Yates, M..G., Swihart, G.H., Moore, P.B. & Marques, N. (1991): The paragenesis of serendibite at Johnsburg, New York, USA: an example of boron enrichment in the granulite facies. *in:* "Progress in metamorphic and magmatic petrology", L.L. Perchuk, ed., Cambridge Univ. Press, Cambridge, UK, 247-285.

Griffen, D.T. & Ribbe, P.H. (1976): Refinement of the crystal structure of celsian. *Am. Mineral.*, **61**, 414-418.

Griffen, D.T., Ribbe, P.H., Gibbs, G.V. (1977): The structure of slawsonite, a strontium analog of paracelsian. *Am. Mineral.*, **62**, 31-35.

Harlow, G.E. (1994): Jadeitites, albitites and related rocks from the Motagua Fault Zone, Guatemala. *J. metamorphic Geol.*, **12**, 49-68.

— (1995): Crystal-chemistry of barian enrichment in micas from metasomatized inclusions in serpentinite, Motagua Fault Zone, Guatemala. *Eur. J. Mineral.*, **7**, 775-789.

Hayob, J.L., Bohlen, S.R., Essene, E.J. (1993) Experimental investigation and application of the reaction rutile + pyroxene = quartz + ilmenite. *Contrib. Mineral. Petrol.*, **115**, 18-37.

Hoffman, V. & Novak, F. (1966): Axinite and barium-adularia from Chvaletice in the Zelezne Hory. *Sbornik Narodniho Muzea Praze, Rada B* **22**, 27-46.

Hori, H., Nakai, I., Nagashima, K., Matsubara, S., Kato, A. (1987) Stronalsite $SrNa_2Al_4Si_4O_{16}$, a new mineral from Rendai, Kochi City, Japan. *Mineral. J.*, **13**, 368-375.

Jakobsen, U.H. (1990): A hydrated barium silicate in unmetamorphosed sedimentary rocks of central North Greenland. *Mineral. Mag.*, **54**, 81-89.

Kalinin, P.V. (1939): Hyalophane from the Slyudyanka River. *Dokl. Akad. Nauk SSSR*, **23**, 163-164.

Kastner, M. & Siever, R. (1979): Low temperature feldspars in sedimentary rocks. *Am. J. Sci.*, **279**, 435-479.

Kato, A., Matsubara, S., Watanabe, T. (1987): Banalsite and serandite from the Shiromaru Mine, Tokyo. *Bull. Nat. Sci. Mus. Ser. C: Geol. Paleo.*, **13**, 107-114.

Klyavin, V.K. (1973): Decomposition of hyalophane and formation of turquoise in the weathered crust of the southern Bukantau foothills, Central Kyzylkum. *Izv. Akad. Nauk SSSR, Ser. Geol.*, **4**, 136-138.

Korinevsky, V.G. (2004): The first find of hyalophane in the Urals. *Dokl. Earth Sci.*, **395**, 202-205.

Kribek, B., Hladikova, J., Zak, K., Bendl, J., Puudlova, N., Uhlik, Z. (1996): Barite–hyalophane sulfide ores at Rozna, Bohemian Massif, Czech Republic: metamorphosed black shale-hosted submarine exhalative mineralization. *Econ. Geol.*, **91**, 14-35.

Lagache, M. (1993): Na–Ba and K–Ba partitioning between feldspar and aqueous chloride solutions: some consequences of unmixing in solids and fluids. *Eur. J. Mineral.*, **5**, 447-454.

— (1999): Equilibre entre phases du système ternaire: albite, anorthite, feldspath strontique et solution chlorurée à 750°C, 200 MPa. *Comptes Rendus Acad. Sci. Paris, Série II, Sci. Terre Planètes*, **328**, 303-308.

Lagache, M. & Catel, N. (1992): Solid solution and unmixing in the (Ba,K,Na)-feldspars. Part I. The albite–celsian solvus determined by ion-exchange experiments. *Eur. J. Mineral.*, **4**, 209-212.

Lahtinen, R. & Johanson, B. (1987): Barium feldspar from Pukkiharju base-metal mineralization, central Finland. *Bull. Geol. Soc. Finland*, **59**, 77-80.

Langworthy, A.P. & Black, L.P. (1978): The Mordor Complex: a highly differentiated potassic intrusion with kimberlitic affinities in central Australia. *Contrib. Mineral. Petrol.*, **67**, 51-62.

Larsen, E.S. (1941): Igneous rocks of the Highwood Mountains, Montana. Part II. The extrusive rocks. *Geol. Soc. Am. Bull.*, **52**, 1733-1752.

Larsen, J.G. (1981): Medium pressure crystallization of a monchiquitic magma: evidence from megacrysts of Drever's Block, Ubekendt Ejland, West Greenland. *Lithos*, **14**, 241-262.

— (1982): Mantle-derived dunite and lherzolite nodules from Ubekendt Ejland, west Greenland Tertiary province. *Mineral. Mag.*, **46**, 329-336.

Lee, M.R. & Parsons, I. (2003): Microtextures of authigenic Or-rich feldspar in the Upper Triassic Humber group, UK North Sea. *Sediment.*, **50**, 597-608.

Lin, H.C. & Foster, W.R. (1968): Studies in the system BaO–Al_2O_3–SiO_2. I. The polymorphism of celsian. *Am. Mineral.*, **53**, 134-144.

Long, H., Long, J., Zhong, Y., Zhuang, S., Liu, T. (1994): Existence of hyalophanite in the Zhangcun-Zhengfang black shales vanadium deposit: evidence for a hydrothermal genesis. *Chin. Sci. Bull.*, **39**, 1024-1827.

Marchenko, E.Y. (1980): Hyalophane from desiliconized pegmatites of the Azov sea area Pre-Cambrian. *Dokl. Akad. Ukr. SSR*, **5**, 27-31.

— (1998): Celsian feldspars: indicators of rock and ore formation. *Mineral'ni Resursi Ukrayini, Naukovo-Prosvitniy Zh.*, **3**, 3-5.

Maruyama, S., Liou, J.G., Suzuki, K. (1982): The peristerite gap in low-grade metamorphic rocks. *Contrib. Mineral. Petrol.*, **81**, 268-276.

Mason, B. (1987): Armenite from Broken Hill, Australia, with comments on calciocelsian and barium anorthite. *Mineral. Mag.*, **51**, 317-318.

Matsubara, S. (1985): The mineralogical implication of barium and strontium silicates. *Bull. Nat. Sci. Mus. Tokyo Ser. C*, **11**(2), 1-95.

McSwiggen, P.L., Morey, G.B., Cleland, J.M. (1994): Occurrence and genetic implications of hyalophane in manganese-rich iron-formation, Cuyuna Iron Range, Minnesota, USA. *Mineral. Mag.*, **58**, 387-399.

Meier, A.E. & Tomlinson, W.H. (1939): An association of harmotome, corundum, and hyalophane at Glen Riddle, Pennsylvania. *Am. Mineral.*, **24**, 189.

Melcher, F. (1995): Genesis of chemical sediments in Birimian greenstone belts: evidence from gondites and related manganese-bearing rocks from N. Ghana. *Mineral. Mag.*, **59**, 229-251.

Melluso, L., Morra, V., di Girolamo, P. (1996): The Mt. Vulture volcanic complex (Italy): evidence for distinct parental magmas and for residual melts with melilite. *Mineral. Petrol.*, **56**, 225-250.

Mezger, K., van der Pluijm, B.A., Essene, E.J., Halliday, A.N. (1993): Thermochronology of the southern Grenville orogen in Ontario, Canada. *Contrib. Mineral. Petrol.*, **114**, 13-26.

Middlemost, E.A.K., Paul, D.K., Fletcher, I.R. (1988): Geochemistry and mineralogy of the minette-lamproite association from the Indian Gondwanas. *Lithos*, **22**, 31-42.

Milliken, K.L. (1992): Chemical behavior of detrital feldspars in mudrocks vs. sandstones, Frio Formation, S Texas. *J. Sediment. Petrol.*, **62**, 790-801.

Morad, S., Marfil, R., de la Pena, J.A. (1989): Diagenetic K-feldspar pseudomorphs in the Triassic Buntsandstein sandstones of the Iberian Range, Spain. *Sediment.*, **36**, 635-650.

Moro, M.C., Cembranos, M.K., Fernandez, A. (2001): Celsian, (Ba,K)-feldspar and cymrite from sedex barite deposits of Zamora, Spain. *Can. Mineral.*, **39**, 1039-1051.

Moya Corral, J.S. & Verduch, A.G. (1978): The solid solution of silica in celsian. *Trans. J. Brit. Ceram. Soc.*, **77**, 40-44.

Nakamura, Y. & Yoder, H.S. Jr. (1974): Analcite, hyalophane, and phillipsite from the Highwood Mountains, Montana. *Carnegie Inst. Wash. Yrbk.*, **73**, 354-358.

Nakano, S. (1977): On the texture of barium-containing alkali feldspars from the Taguchi Mine, Aichi Prefecture, Japan. *Mineral. J.*, **8**, 361-373.

— (1979): Intergrowth of barium microcline, hyalophane and albite in the barium-containing alkali feldspar from the Noda-Tamagawa Mine, Iwate Prefecture, Japan. *Mineral. J.*, **9**, 409-416.

Nemec, D. (1975): Barium in K-feldspar megacrysts from granitic and syenitic rocks of the Bohemian Massif. *Tschermaks Mineral. Petrogr. Mitt.*, **22**, 109-116.

Nkoumbou, C., Deruelle, B., Velde, D. (1995): Petrology of Mt Etinde nephelinite series. *J. Petrol.*, **36**, 373-395.

Nockolds, S.R. & Zies, E.G. (1933): On a new barium plagioclase feldspar. *Mineral. Mag.*, **23**, 448-457.

Novak, F. & Hoffman, V. (1960): Hyalophane from Chvaletice. *Vestnik Ustredniho Ustavu Geologickeho*, **35**, 143-149.

Pan, Y. & Fleet, M.E. (1991): Barian feldspar and barian-chromian muscovite from the Hemlo area, Ontario. *Can. Mineral.*, **29**, 481-498.

Pautov, L.A., Agakhanov, A.A., Sokolova, E., Hawthorne, F.C. (2004): Maleevite, $BaB_2Si_2O_8$, and pekovite, $SrB_2Si_2O_8$, new mineral species from the Dara-i-Pioz alkaline massif, northern Tajikistan: description and crystal structure. *Can. Mineral.*, **42**, 107-119.

Peterson, E.U., Anovitz, L.M., Essene, E.J. (1984): Donpeacorite, $(Mn,Mg)MgSi_2O_6$, a new orthopyroxene and proposed phase relations in the system $MnSiO_3$–$MgSiO_3$–$FeSiO_3$. *Am. Mineral.*, **69**, 472-480.

Pivec, E. Jr., Srein, V., Navratil, O. (1990): Hyalophane and Ba-muscovite in a pegmatite-aplite vein from Krhanice, central Bohemia, Czechoslovakia. *Acta Univ. Carol. Geol.*, 131-140.

Polgári, M. & Fórizs, I. (1996): Distribution of Mn in carbonates of the Uppony Mts., N.E.-Hungary. *Geol. Carpathica*, **47**, 215-225.

Rathmell, M.A. (1993): Comparison of garnet–biotite, calcite–graphite and calcite–dolomite thermometry in the Grenville Orogen, Canada. MSc thesis, Univ. Michigan, 99 p.

Rathmell, M.A., Streepey, M.M., Essene, E.J., van der Pluijm, B.A. (1999): Comparison of garnet–biotite, calcite–graphite and calcite–dolomite thermometry in the Grenville Orogen, Canada. *Contrib. Mineral. Petrol.*, **134**, 217-231.

Reinecke, T. (1982): Cymrite and celsian in manganese-rich metamorphic rocks from Andros Island/Greece. *Contrib. Mineral. Petrol.*, **79**, 333-336.

Riley, T.R. & Bailey, D.K. (2003): Barium-rich sanidine megacrysts from the West Eifel (Germany). *N. Jb. Mineral. Monat.*, 2003, 18-30.

Roy, N.N. (1965): The mineralogy of the potassium-barium feldspar series. II. Studies on hydrothermally synthesized members. *Mineral. Mag.*, **36**, 43-49.

Saigal, G.C., Morad, S., Bjørlykke, K., Egeberg, P.K., Aagaard, P. (1988): Diagenetic albitization of detrital K-feldspar in Jurassic, Lower Cretaceous and Mesozoic clastic reservoir rocks from offshore Norway. I. Textures and origin. *J. Sediment. Petrol.*, **58**, 1003-1013.

Schmädicke, E., Okrusch, M., Schmidt, W. (1992): Eclogite-facies rocks in the Saxonian Erzgebirge, Germany: high pressure metamorphism under contrasting P-T conditions. *Contrib. Mineral. Petrol.*, **110**, 226-241.

Segnit, E.R. (1946): Barium-felspars from Broken Hill, New South Wales. *Mineral. Mag.*, **27**, 166-174.

Shramenko, I.F., Stadnik, V.O., Kostyuchenko, V.S. (1980): Celsian mineralization in rocks of the Pliskovian Structure. *Dopov Akad. Nauk Ukr. RSR, Ser. B: Geol., Khim. Biol. Nauki*, **4**, 22-25.

Skellern, M.G., Howie, R.A., Lachowski, E.E., Skakle, J.M.S. (2003): Barium-deficient celsian, $Ba_{1-2x}Al_{2+2x}Si_{3+x}O_8$. *Acta Cryst. C*, **59**, I11-I14.

Smith, J.V. (1983): Phase equilibria of plagioclase. *in:* "Feldspar mineralogy", 2nd. ed., Ribbe, P.H., ed., *Rev. Mineral.*, **2**, 281-323.

Spencer, L.J. (1942): Barium felspars (celsian and paracelsian) from Wales. *Mineral. Mag.*, **26**, 231-245.

Streepey, M., Essene, E.J., van der Pluijm, B.A. (1997): A compilation of thermobarometric data from the Metasedimentary Belt, Grenville Province, Ontario and New York. *Can. Mineral.*, **35**, 1237-1248.

Tropper, P., Manning, C.E., Essene, E.J. (2002): The substitution of Al and F in titanite at high pressure and temperature: experimental constraints on phase relations and solid solution properties. *J. Petrol.*, **43**, 1787-1814.

Tsyganov, A.A. & Vrublevskaya, T.T. (1998): The nature of the anomalous Ba contents in Riphean granitoids of the island-arc type in eastern Siberia. *Geochem. Internat.*, **36**, 1123-1132.

Vermaas, F.H.S. (1953): A new occurrence of barium-feldspar at Otjosondu, South-West Africa, and an X-ray method for determining the composition of hyalophane. *Am. Mineral.*, **38**, 845-857.

Viswanathan, K. (1978): Intergrowth of Ba-rich and Ba-poor phases in barium feldspars from Otjosondu, South-West Africa. *Mineral. Mag.*, **42**, 294.

Viswanathan, K. (1992): Solid solution and unmixing in the (Ba,K,Na)-feldspars. Part II: An X-ray powder diffraction study of the ternary feldspars. *Eur. J. Mineral.*, **4**, 213-216.

Viswanathan, K. & Harneit, O. (1989): Solid-solution and unmixing in the feldspar system, albite ($NaAlSi_3O_8$)–celsian ($BaAl_2Si_2O_8$). *Eur. J. Mineral.*, **1**, 239-248.

Viswanathan, K. & Kielhorn, H.-M. (1983a): Variations in the chemical compositions and lattice dimensions of (Ba,K,Na)-feldspar from Othosondu, Namibia and their significance. *Am. Mineral.*, **68**, 112-121.

—,— (1983b): Al, Si distribution in a ternary (Ba,K,Na)-feldspar as determined by crystal structure refinement. *Am. Mineral.*, **68**, 121-124.

Walker, T.R. (1984): Diagenetic albitization of potassium feldspar in arkosic sandstones. *J. Sediment. Petrol.*, **54**, 3-16.

Wen, S. & Nekvasil H. (1994): SOLVCALC: an interactive graphic program package for calculating the ternary feldspar solvus and for two-feldspar geothermometry. *Computers Geosci.*, **20**, 1025-1040.

Wenk, E. & Wenk, H.-R. (1984): Distribution of plagioclase in carbonate rocks from the Tertiary metamorphic belt of the Central Alps. *Bull. Minéral.*, **107**, 357-368.

Wenk, E., Schwander, H., Wenk, H.-R. (1986): Alkali feldspar and coexisting plagioclase in metamorphic carbonate rocks from the Central Alps. *N. Jb. Mineral. Abh.*, **155**, 89-108.

—,—,— (1991): Microprobe analyses of plagioclases from metamorphic carbonate rocks of the Central Alps. *Eur. J. Mineral.*, **3**, 181-191.

Wilkinson, J.F.G. (1968): Analcimes from some potassic igneous rocks and aspects of analcime-rich igneous assemblages. *Contrib. Mineral. Petrol.*, **18**, 252-269.

Woods, M.J. (1976): Fractionation and origin of the Highwood Mountain volcanic rocks (Montana). *NW Geol.*, **5**, 1-9.

Yan, Y., Li, W., Sills, J.D. (1991): Some rare rocks in Archaean Caozhuang Group and their geological significance in Qian'an, Hebei. *Acta Petrol. Sinica*, 19-27.

Yanev, Y., Stoykov, S., Pechkay, Z. (1998): Petrology and K-Ar dating of the Paleogene magmatism in the region of the villages Yabalkov and Stalevo, eastern Rhodopes volcanic area. *Geokhim., Mineral., Petrol.*, **34**, 97-110.

Yosimura, T. (1939): Studies on the minerals from the manganese deposit of the Kaso Mine, Japan. *J. Fac. Sci., Hokkaido Univ., Ser. 4: Geol. Mineral.*, **4**, 316-451.

Yui, T.F., Lo, C.-H., Lee, C.W. (1989): Mineralogy and petrology of metamorphosed manganese-rich rocks in the area of Santzan River, eastern Taiwan. *N. Jb. Mineral. Abh.*, **160**, 249-268.

Zak, L. (1991): Hyalophane-zoisite veins from the pyrite-rhodochrosite deposits near Litosice in eastern Bohemia (Czechoslovakia). *Casopis Mineral. Geol.*, **36**, 67-75.

Zaslavskiy, B.I., Krupnyy, A.I., Aleksandrov, K.S. (1974): Elastic properties of rock-forming minerals. VII. Hyalophane and danburite. *Izv. Earth Phys.*, **8**, 55-58.

Zebec, V. & Bermanec, V. (1985): Albite and oriented intergrowth between hyalophane and albite from Zagrade near Busovaca in Bosnia [Yugoslavia]. *Geol. Vjesn.*, **38**, 115-119.

Zhang, M., Suddaby, P., Thompson, R.N., Dungan, M.A. (1993): The origins of contrasting zoning patterns in hyalophane from olivine leucitites, NE China. *Mineral. Mag.*, **57**, 565-573.

Received 17 June 2003
Modified version received 10 December 2004
Accepted 31 January 2005